*This is the accepted version of the following article: Machine Learning for Bioelectronics on Wearable and Implantable Devices: Challenges and Potential, which has now been formally published in final form at Tissue Engineering Part A at [https://doi.org/10.1089/ten.tea.2022.011](https://doi.org/10.1089/ten.tea.2022.011). This original submission version of the article may be used for non-commercial purposes in accordance with the Mary Ann Liebert, Inc., publishers' self-archiving terms and conditions.*

# Machine learning for bioelectronics on wearable and implantable devices: challenges and potential

Guo Dong Goh[1], Jia Min Lee[2], Guo Liang Goh[3], Huang Xi[2], Samuel Lee[3], Wai Yee Yeong[1,3]*

[1]Singapore Centre for 3D Printing, School of Mechanical & Aerospace Engineering, Nanyang Technological University Singapore, 50 Nanyang Avenue, Singapore 639798

[2]NTU-HP joint lab, Nanyang Technological University Singapore, 50 Nanyang Avenue, Singapore 639798

[3]Schaeffler Hub for Advanced Research (SHARE@NTU), Nanyang Technological University Singapore, 61 Nanyang Drive, Singapore 637460

*Corresponding Author

Designation:

Associate Professor, School of Mechanical and Aerospace Engineering, Nanyang Technological University, Singapore

Email: WYYeong@ntu.edu.sg

Tel: (+65) 6790 5130

**Keywords:**

Data Science; integrated system; bioprinting; 3D printing

## Abstract

Bioelectronics presents a promising future in the field of embedded and implantable electronics, providing a range of functional applications, from personal health monitoring to bioactuators. However, due to the intrinsic difficulties present in producing and optimising bioelectronics, recent research has focused on utilising machine learning to reliably mitigate such issues and aid in process development. This review focuses on the recent developments of integrating machine learning into bioelectronics, aiding in a multitude of areas such as: material development, fabrication process optimisation and system integration. First, discussing how machine learning has aided in the materials development by identifying complex relationships between process input parameters and desired outputs, such as product design. Second, examine the advancements in machine learning to accurately optimise fabrication precision and stability for various 3D printing technologies. Third, provide an overview of how machine learning can greatly assist in the analysis of complex, non-linear relationships in data obtained from bioelectronics. Lastly, a summary of the challenges present with utilising machine learning with bioelectronics and any other developments in this field. Such advancements in the field of bioelectronics and machine learning could hopefully build a strong foundation for this research field, promoting smart optimisation together with effective use of machine learning to further enhance the effectiveness of such applications.

**Impact statement**:

The article serves to give insight about the use of the machine learning techniques in the field of bioelectronics. Since bioelectronics and machine learning are two distinct fields. This paper allows bioelectronics researcher to get to know the latest advancement in the machine learning field. On the other hand, the paper provides an insight to the machine learning researchers about how machine learning techniques can be useful in bioelectronics applications.

## 1. Introduction

Bioelectronics describe a discipline that crosses over between electronics and biological systems. The field can be broadly categorised into actuators and sensors, targeting biological systems from micro to macro level. From cell to tissue/organ and even to the macroscale movement of muscles, development of bioelectronics at different scale level is growing rapidly. The boundary that highlight bioelectronics from micro/nano electro-mechanical devices is when the former is a biological or biochemical forward device. Energy harvester, also known as triboelectric nanogenerator, scavenges human body energy as useful electrical power (1, 2)

Bioelectronics, that are intend to receive information from the biological system, are designed to function as recording devices or sensors capturing the electrochemical changes in cells/tissues. For instance, cells in the nervous system communicates based on ionic fluxes, which can be detected as electrical potentials by the electrodes. Soft bioelectronics with mechanical properties that matches closely with the biological tissues are widely used such as the metabolite sensing for personal health monitoring and electrophysiological recording.

*This is the accepted version of the following article: Machine Learning for Bioelectronics on Wearable and Implantable Devices: Challenges and Potential, which has now been formally published in final form at Tissue Engineering Part A at https://doi.org/10.1089/ten.tea.2022.011. This original submission version of the article may be used for non-commercial purposes in accordance with the Mary Ann Liebert, Inc., publishers' self-archiving terms and conditions.*

Multi-functional bioelectronics, specifically in the form of wearable and implantable devices, have gained research interests as theragnostic tools in modern healthcare (3-6). Self-powered sensing platforms that harvest energy from motion (e.g. heartbeat, respiration) or chemical reaction (e.g. redox reaction) (5, 7, 8). Transient technology is an emerging class within bioelectronics that focuses on degradable devices and systems. The interest lies in implanting these devices for a specific timeframe, and eventually resolve into biological system without the need of secondary surgeries for removal. In transient bioelectronics, biodegradable polymeric materials form the substrate material as it interfaces better with biological tissue. These polymers can be either natural (e.g. silk, collagen, alginate, chitosan, decellularized matrices) or synthetic (e.g. PGA, PLA, PLGA, PCL, PVA) (9-16). On the other hand, biodegradable metals, such as magnesiuim, iron, zinc and their alloys, are explored for its use as the electronic components of these transient devices (10, 11, 15-18). For reviews on materials and systems for biodegradable electronics, readers are referred to the following articles (19-24).

Machine learning has been used to improve the design and fabrication process in bioelectronics with the help of large dataset and the constantly improving computing power. In this review, we provide a brief introduction on the different machine learning approaches. Next, we identify key areas in which machine learning can broaden the field of bioelectronics specifically in material development, fabrication process optimization and system integration. We first identify the "What" in aspect of materials used in bioelectronics as wearable and implantable devices. Secondly, we discuss the "How" in terms of fabricating bioelectronics. We will highlight key processes used for fabricating electronics and bioelectronics. Thirdly, we demonstrate how machine learning are introduced in the three aspects: material development, process optimization, and system integration.

## 2. Machine Learning Techniques

Machine learning is a powerful tool that can extract useful information efficiently from large datasets. Machine learning is a subset of artificial intelligence which can learn from existing data to make decision on new data. Through iteration of algorithms, machine learning techniques identify the statistical relationship between the fed data, resulting in a generalized model which can be used to predict the result of new input. There are three basic approaches to machine learning, supervised learning (25), unsupervised learning (26, 27), and reinforcement learning (28-30). The flowchart depicting the steps for these approaches is visualized in Figure 1 (a), while the examples are shown in Figure 1 (b).

Supervised learning is the most used approach of machine learning. The algorithm draw relationship from existing data with labeled output, which is then used to predict the output for given input. Two common usage of supervised learning is in regression and classification. In regression, an output value can be predicted from the input, such as predicting the housing price from the given number of rooms, size of each room, availability of garden, and the location of the property. In classification, the output is a class instead of a value, such as in image recognition to identify the object in the image, or to detect if an email is a spam. Examples of supervised learning algorithm are linear regression, logistic regression, support vector machine (31), decision trees (32), random forest (33), artificial neural network (ANN) (34, 35), naive Bayes (36), AdaBoost (37), and ensemble method (38). Table 1 highlights the advantages and disadvantages of various supervised learning techniques

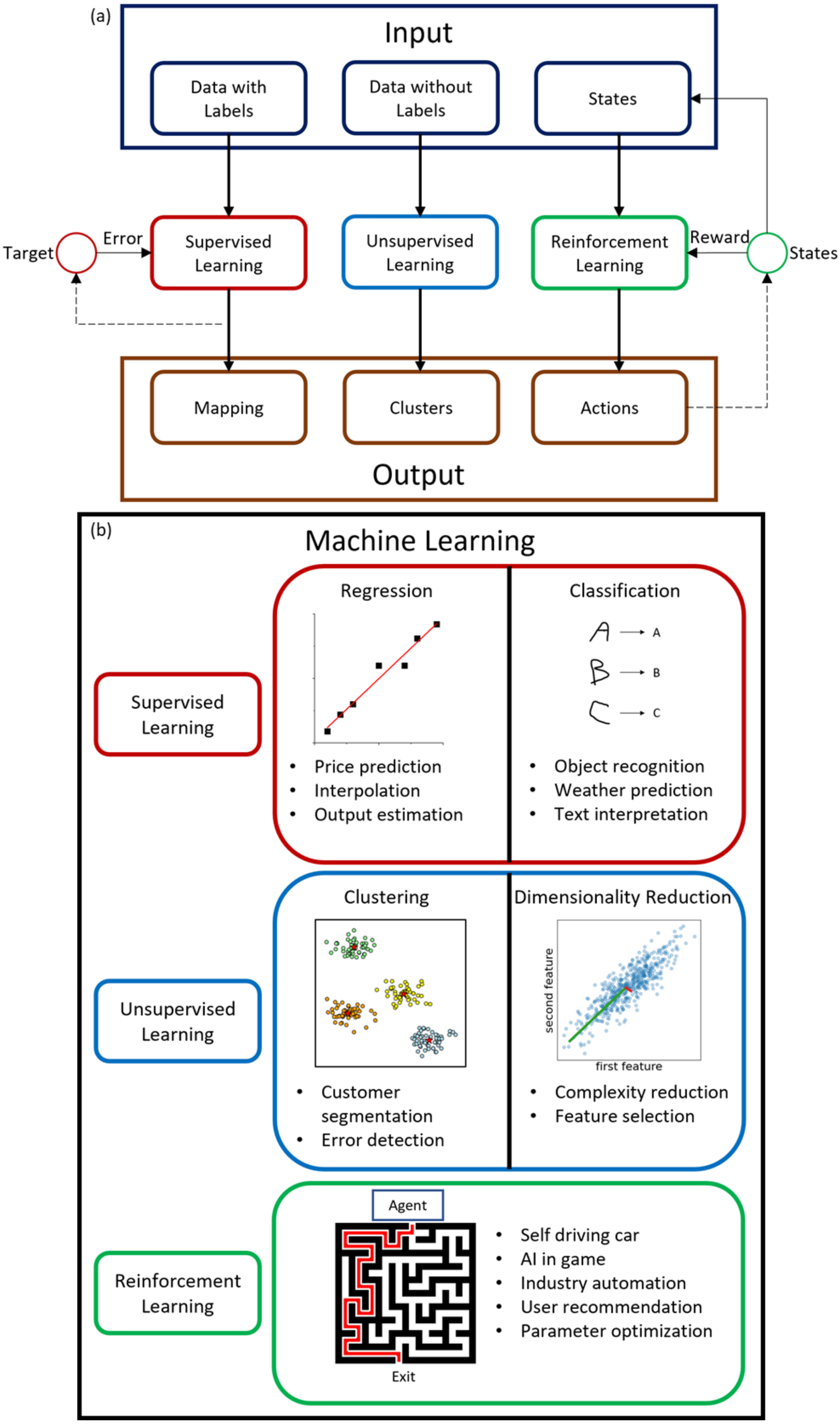
(a)
Input
Data with Labels
Data without Labels
States
Target
Error
Supervised Learning
Unsupervised Learning
Reinforcement Learning
Reward
States
Mapping
Clusters
Actions
Output
(b)
Machine Learning
Supervised Learning
Regression
Price prediction
Interpolation
Output estimation
Classification
Object recognition
Weather prediction
Text interpretation
Unsupervised Learning
Clustering
Customer segmentation
Error detection
Dimensionality Reduction
second feature
first feature
Complexity reduction
Feature selection
Reinforcement Learning
Agent
Exit
Self driving car
AI in game
Industry automation
User recommendation
Parameter optimization

*Figure 1: (a) Flowchart for supervised learning, unsupervised learning, and reinforcement learning. (b) Examples for various approaches of machine learning*

*Table 1 Summary of various supervised learning techniques*

| Supervised Learning Techniques | Type | Advantages | Disadvantages |
|---|---|---|---|
| Linear/Polynomial Regression | Regression | Easy to implement.<br>Fast training time.<br>Resultant model is easy to understand. | Inaccurate if the data does not have a linear or polynomial relationship. |
| Logistic Regression | Classification | Easy to implement.<br>Fast training time.<br>Resultant model is easy to understand. | Inaccurate if the data have a complex relationship.<br>Can easily overfit.<br>Generic logistic regression will only differentiate between 2 categories. |
| Support Vector Machine (SVM) | Classification | Lower risk of overfitting when compared to logistic regression.<br>Resultant model is easy to understand. | Computationally expensive.<br>Generic SVM will only differentiate between 2 categories. |
| Decision Trees | Regression/Classification | Can differentiate between multiple categories.<br>Resultant model is easy to understand. | Will be overfit easily with non-optimal parameters.<br>Unstable.<br>Bad at extrapolation. |
| Naive Bayes | Classification | Low sample size needed.<br>Good for large datasets.<br>Usable for both binary and multi-class datasets.<br>Less prone to overfit.<br>Fast training time. | Assume that classes are mutually exclusive.<br>May have wrong prediction where there are unfamiliar features to a class. |
| Ensemble Method | Regression/Classification | Very high accuracy compared to all the previous models.<br>Can describe datasets with multiple models involved. | Computationally expensive.<br>Difficult to implement.<br>Difficult to interpret. |

| | | | |
|---|---|---|---|
| Random Forest | Regression/Classification | Ensemble method for decision trees. Higher accuracy and less prone to overfitting than decision trees.<br>Good for large datasets.<br>Training can be parallelized. | Computationally expensive.<br>The resultant model is very complex and difficult to read. |
| Adaboost | Regression/Classification | Ensemble method for decision trees.<br>More accurate than Random Forest. | Computationally expensive.<br>Bad at generalizing noisy data. |
| Artificial Neural Network (ANN) | Regression/Classification | Can detect complex relationship between datasets.<br>Easy to implement.<br>Modular and high expandability.<br>Can learn from previous knowledge (transfer learning). | The resultant model is usually a black box and has very low readability.<br>Computationally expensive for complex model. |

Unsupervised learning extracts the features out of the unlabeled dataset for various purposes such as clustering them into multiple groups or for dimensionality reduction. This technique is commonly used in classifying the customer into different groups based on their similarity, identifying particles in a microscopy image, anomaly detection, and reducing the amount of input variables in a dataset by identifying the more important features. Examples of unsupervised learning algorithms are K-means (39, 40), principal component analysis (PCA) (41-43), and singular value decomposition (SVD) (44). Table 2 highlights the advantages and disadvantages of various unsupervised learning techniques

*Table 2 Summary of various unsupervised learning techniques*

| Name | Type | Advantages | Disadvantages |
|---|---|---|---|
| K-Means | Clustering | Simple to implement.<br>Scalable to large datasets. | Number of clusters (k) have to be manually chosen before starting the training.<br>Affected by outliers. |
| Principal Component Analysis (PCA) | Dimensionality Reduction | PCA is used before other ML methods to:<br>• Remove correlated features. | Some information is removed after PCA.<br>Lower readability for ML models because the original features are not retained. |

| | | | |
|---|---|---|---|
| | | • Reduces overfitting.<br>• Improve performance of training. | |
| Singular Value Decomposition (SVD) | Dimensionality Reduction | Can be used in multiple fields.<br>• Solution to linear equations.<br>• Filter of noisy signals.<br>• Time series analysis. | Computationally expensive. |

Reinforcement learning is an approach where the algorithm maximizes the cumulative reward function. While in supervised learning the prediction is compared to the correct output, in reinforcement learning has a reward function to quantify how successful is the current output or decision instead. The algorithm optimizes its decision after every iteration. Unlike supervised learning and unsupervised learning where the inference is made after the training is completed, the training can be continued during usage in reinforcement learning to improve the model. A few examples of reinforcement learning are the translation program, self-driving car, AI for board game such as AlphaGo (45), and automation in industry. The algorithms commonly used for reinforcement learning are Markov decision process (46), Q-learning (47), Monte Carlo, and deep reinforcement learning (28). Table 3 highlights the pros and cons of the various reinforced learning techniques.

*Table 3 Summary of the various reinforced learning techniques*

| Reinforced learning techniques | Types | Advantages | Disadvantages |
|---|---|---|---|
| Markov Decision Process | Reinforcement Learning | Learn the best strategy when the probability of each action is known. | Not usable when there are undefined probabilities, rewards, or penalties. |
| Q-Learning | Reinforcement Learning | Learn the best strategy when some probabilities, rewards, and penalties are unknown. | Only works if the environment is discrete and finite. |
| Monte Carlo | Reinforcement Learning | Estimate the full range of potential outcomes in a model. | Computationally expensive. |

*This is the accepted version of the following article: Machine Learning for Bioelectronics on Wearable and Implantable Devices: Challenges and Potential, which has now been formally published in final form at Tissue Engineering Part A at https://doi.org/10.1089/ten.tea.2022.011. This original submission version of the article may be used for non-commercial purposes in accordance with the Mary Ann Liebert, Inc., publishers' self-archiving terms and conditions.*

| | | | |
|---|---|---|---|
| Deep Reinforcement Learning | Reinforcement Learning | Scalable and modular. Have higher accuracy in complex problems. | Computationally expensive for complex model. The resultant model is a black box. |

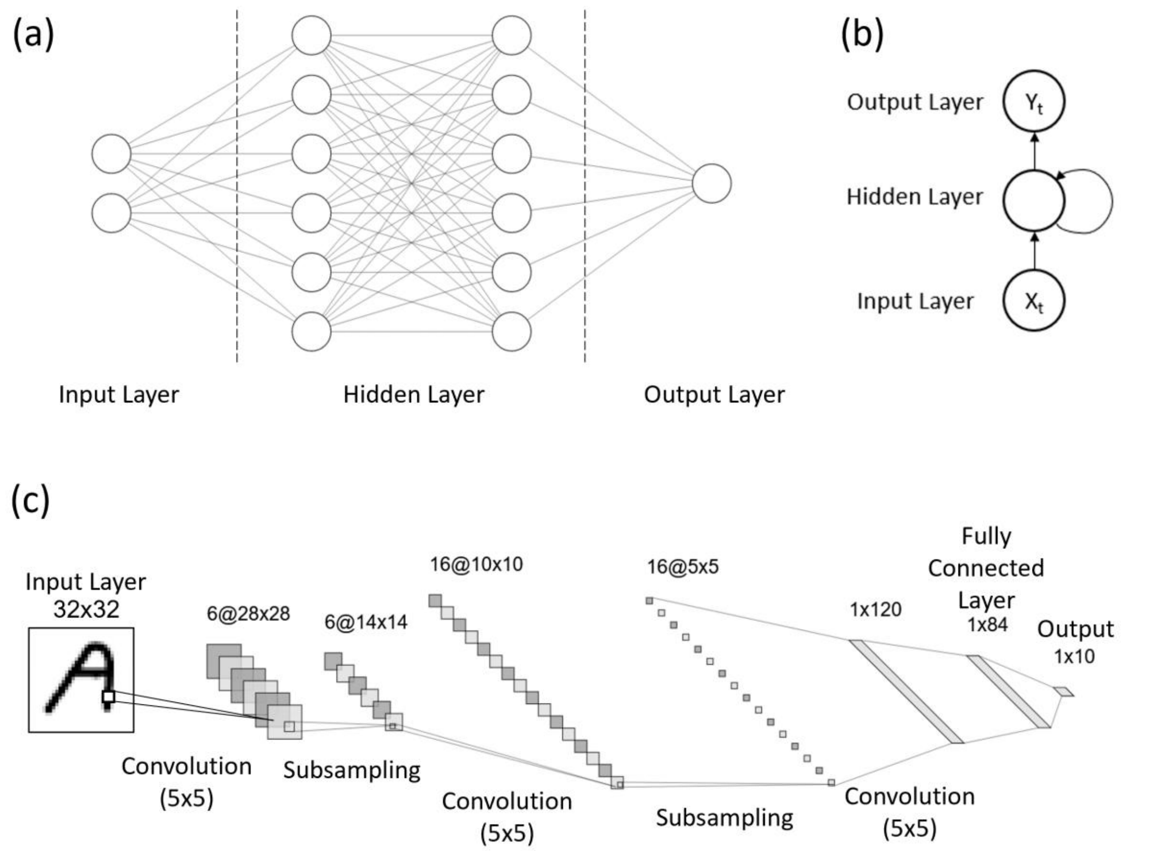


*Figure 2 (a) Schematic for deep neural network (DNN). (b) Schematic for recurrent neural network (RNN). (c) Schematic for convolutional neural networks (CNN), the architecture shown is LeNet-5 (48).*

Aside from the classical machine learning technique, deep learning is a booming sub field of machine learning as it can take advantage of the dramatic increase in the computational power and the availability of massive data (49). Deep learning outperforms classical machine learning technique in many applications, such as in image (50-52), speech recognition (53, 54), natural language processing (55), and translation (56). Deep learning use multiple neuron layers to process the input, which each layer containing simple but nonlinear module to transform the representation from previous layer into a more abstract representation at higher level (49). By rearranging the modules, deep learning can process a wide variety of data for different purposes. For example, deep neural network (DNN) can accept multiple variables and correlate it to single or multiple outputs (49), convolutional neural network (CNN) is able to extract feature from spatial relation between data such as images (57), recurrent neural network (RNN) can store state from previous input to process a series of data such as time series, sentences, or speech recognition (58). Schematics for DNN, RNN, and CNN is shown in Figure 2. The comparison of classical machine learning and deep learning is demonstrated in Table 4.

*Table 4: Advantages and disadvantages of classical machine learning and deep learning.*

| | Classical Machine Learning | Deep Learning |
|---|---|---|
| Advantages | Fast.<br>Require low sample size. | Good scalability.<br>Remarkably modular.<br>Higher accuracy when large sample size is given. |
| Disadvantages | Low scalability. | Lower performance compared to classical machine learning at low sample size. |

## 3. Materials, Process, System in Bioelectronics

### *3.1 Materials in Bioelectronics*

Mechanical mismatch between implants and tissues can result in failure of devices, as in the case of implantable devices. Similarly in tissue engineering application, one of the critical consideration in engineering biomaterials is to match mechanical compliance with host tissue. Polymeric materials such as polyimide (59, 60), parylene C (61-63), and Polydimethylsiloxane (PDMS) (63, 64) have been used to reduce the modulus gap between tissue and devices. However, these polymeric materials with Young's moduli of MPa to GPa differs to biological tissue in the kPa to MPa range (65). As such, hydrogels have attracted growing interest as substrates with conformability and similarity to biological tissues for use in bioelectronic (65). Synthetic hydrogel such as Polyacrylamide (PAm), polyvinyl alcohol (PVA), polyacrylic acid (PAAc) have been widely used in bioelectronics (66).

Conformal and stable attachment between bioelectronic device and target tissue is essential, which has been shown to be generally limited to thin devices of less than 5 μm thick with the use of hydrogel as substrate materials for bioelectronic devices. However, recent advancements have allowed for a larger variation in dimensionality of hydrogel substrates(67) while retaining high patterning resolutions (68). Notably, Won et al. have demonstrated a wide range of tuneable variables within conductive hydrogel layers(68) by utilising a mixture of polyvinyl pyrrolidine (PVP) stabilisers and gold nanoparticles (AuNPs) within a poly(3,4-ethylenedioxythiophene):poly(styrene sulfonate) (PEDOT:PSS) hydrogel substrate.

Pairing this with the improvements in nanowire stability, especially in copper-based nanowires (69), and unique bioelectronic designs such as kirigami-inspired flexible electronics (70), a high degree of control can be attained in mechanical properties of bioelectronics while not compromising on biocompatibility. Recent studies such as gold-coated copper nanowires(71) or gold-coated polyurethane nanowires (72) are good examples of newer composite nanowires that could also be incorporated into such hydrogels.

Encapsulation of hydrogel is used to prevent drying of gel which impacts its resistivity and geometry. Sai devised a strategy that incorporates polyurethane monomers in hydrogel as mixture, which upon ultraviolet (UV) irradiation forms a skin-like interface that protects the hydrogel from its environment (73). The electrical conductivity of hydrogel was preserved with the present of polyurethane skin.

Bioadhesives have been researched to mitigate challenges at the interface of bioelectronic devices with tissues and organs. Other than conformability of hydrogel with the geometry of surface, the interfacial adhesion between hydrogels and biological tissues ensures that there is close contact between bioelectronic device and the biological system. Hydrogels with functional groups such as hydroxyl, ether, amino, carboxyl or catechol groups, form good adhesiveness with tissue surfaces through imine, amide or other covalent bonds. Other non-covalent interactions, such as hydrogen bonding, π–π interactions, and mechanical interlocking, also offers ways to improve performance of bioelectronic (74). Some considerations for formulating bioadhesives are the performance under wet environment, rapid adhesion formation process, ease of handling, high electrical conductivity and low impedance.

Conductive hydrogels used in bioelectronics are broadly classified into ion-conductive and electro-conductive (75). Mobile ions present in ion-conductive hydrogels are introduced with salt, acid or ionic liquids. Ionic movement in these conductive hydrogel is similar to ion transportation in biological tissue. On the other hand, electro-conductive hydrogel comprises of either intrinsically conductive polymers such as polyaniline (PANI), Poly(3,4-

ethylenedioxythiophene):poly(styrene sulfonate) (PEDOT:PSS), polypyrrole (PPy) or introducing conductive fillers such as carbon nanotubes, graphene, metal nano-/micro-particle into the matrix. One of the challenges in hydrogel-based bioelectronics is the need to prevent drying of gel, thereby preserving its electrical conductivity. Sai devised an encapsulation strategy that incorporates polyurethane monomers in hydrogel as mixture, which upon UV irradiation forms a skin-like interface that protects the hydrogel from its environment (73). This helps preserve the conductivity and integrity of the gel.

Hydrogel remains an attractive material as the substrate for bioelectronics due to its conformability, bioadhesiveness and conductivity. Deng et al showed that hydrogel-based bioelectronics are capable of high electrical conductivity with low impedance at physiologically relevant frequencies (76). The conformal and adhesiveness of device with epicardia tissue allow bidirectional bioelectronic communication and stable epicardial ECG recording of beating heart. Apart from recording and stimulating biomedical devices, hydrogel-based bioelectronics offer an innovative therapeutic solution in healthcare. Kai demonstrated that ionic current from the bioelectronic device, known as bioplaster, accelerated skin wound healing (77). Electrical stimulation promotes cell migration, which enhances the rate of wound closure. Additionally, the hydrogel-based device encourages moist healing, which improves the final appearance of healed skin.

### *3.2 Design and Fabrication of electrodes, sensors, and devices for bioelectronics*

Design and fabrication are closely connected in the development of bioelectronics. Fabrication techniques that efficiently and reliably transfer microelectronic capabilities onto conformable substrate would help advanced development of bioelectronic devices. The overall goal is to have better biointegration at the machine-device interface, bidirectional modalities, and higher spatiotemporal resolution. Microtechnology such as lithography have been paramount to the successful fabrication of these microdevices (78).

Electrodes are essential components for bioelectronics as they are used for electrical stimulation and sensing purposes. Electrical stimulation refers to a process whereby electrical signals such as voltage or current are transmitted to the cells or tissues for purposes such as accelerating the wound healing process, enhancing cell proliferations, and guiding cell alignment. In contrast, bioelectronic sensing refers to a process of acquiring physiological information such as the pH, temperature, and strain from the cells, tissues, or the body for monitoring purposes. Regardless of the types of applications, it is required that the electrodes are electrically conducting so that electrical signals such as voltage and current can be transmitted from or to the host cell/tissues. Usually, these electrodes vary in terms of the electrode materials and the designs depending on the applications. As a result, different fabrication approaches have been developed and utilized for the fabrication of electrodes for bioelectronics. In this section, we will be discussing the different types of materials, designs, and fabrication methods of electrodes for bioelectronics and their respective pros and cons will be elucidated.

Generally, bioelectronics electrodes can be grouped into wet electrodes and dry electrodes, and they are usually flat or 2-dimensional. Depending on the types of the electrodes, the materials and the fabrication methods used will differ. Traditionally, wet electrodes are regarded as the gold standard for electroencephalography (EEG) applications and are widely used in the medical field and scientific laboratory (79). Usually, they are used in applications where liquid electrolytes are required for ion transports or sensing purposes. In this case, the wet electrodes are usually made up of electrically conducting gel that can conform to the skin, therefore enhancing the electrical contact between the skin and the electrode. Conducting gels are usually made up of a mixture of hydrogel and conductive materials such as metal nanoparticles or conductive polymers (80). In general, conducting gels can be prepared in 3 different ways, namely 1) templated conducting hydrogel, 2) deposition of conducting material in hydrogel, and 3) conducting hydrogel formed from a mixture of precursors. The templated conducting hydrogel fabrication method prepares the hydrogel by using a sacrificial material to form nano conduits that allows the conducting material to sip into the hydrogel after the sacrificial material is removed. The second method prepares the conducting hydrogel by first dehydrating the hydrogel to remove the water content and then followed by the absorption of conducting solution by the hydrogel to turn it conducting. In the third method, the hydrogel precursor and the precursor for the conducting material are mixed and then subsequently polymerized together. Despite the wet electrodes are advantageous in terms of the electrical impedance, however, wet electrodes often cause discomfort to the users.

*This is the accepted version of the following article: Machine Learning for Bioelectronics on Wearable and Implantable Devices: Challenges and Potential, which has now been formally published in final form at Tissue Engineering Part A at https://doi.org/10.1089/ten.tea.2022.011. This original submission version of the article may be used for non-commercial purposes in accordance with the Mary Ann Liebert, Inc., publishers' self-archiving terms and conditions.*

Dry electrode, on the other hand, do not have a conducting gel layer, thus giving better comfort to the users when wearing the electrodes (79). In fact, dry electrodes do not work in absolute dryness as sweat and electrolytes from the skin is always present, thus reducing the skin impedance. Dry electrodes are usually made up of conductive materials and they can be produced using different fabrication techniques such as layered coating (81), wet etch method (82), maskless photolithography (83), photon based direct patterning using laser (84-86), intense pulsed light (IPL) (87) and 3D printing (88). Comparing to wet electrodes, dry electrodes usually suffer from high skin/electrode impedance which brings about negative impact on the performance of the electrodes. Besides, dry electrodes are prone to noise due to the poor contact with the skin. Therefore, a semi-dry electrode seems to be a promising option to achieve low skin impedance and good user comfort. Semi-dry electrode designs usually contain a small reservoir to contain a small about of saline that can be released to the skin interface at a controlled rate. Porous ceramic material can be used in the wet electrode to control and release the saline to the conductive gel from the reservoir.

Conventionally, the designs of the electrode and sensors are generally planar or 2-dimensional. Such planer electrode and sensor designs have restrictions in terms of achieving high level of conformity and additional sensing dimension. To overcome the shortcomings conventional planar electrodes, researchers have been exploring various types of 3D electrode designs so that the electrode can reach deeper regions of various 3D tissues (89). In general, microneedle design is usually used for 3D electrodes due to its ability to penetrate deeper into the tissues for sensing and stimulation purposes. Due to biocompatible issue, only some noble metals such as platinum, iridium, and gold can be utilized as the electrode materials for 3D electrodes (90). Other potential materials for 3D electrodes include iridium oxide, titanium nitride, carbon nanotube, graphene, and silicone, just to name a few (89). However, due to the mismatch in young's modulus and toxicity of these materials, they are not suitable for long-term applications in human body. Therefore, polymers such as Parylene-C are usually used as a sheath layer to protect the tissues from coming in contact directly with the electrodes. Alternatively, conducting polymers such as poly (3,4-ethylenedioxythiophene) (PEDOT) or poly(pyrrole) can be used due to their high chemical stability, biocompatibility, and good electrical conductivity. 3D electrodes can be fabricated by either using various fabrication techniques such as photolithography process or 3D printing process. Photolithography process is a subtractive manufacturing method where the patterning of electrode materials is achieved through chemical/physical etching steps. The process is suitable for the fabrication of sub-micrometer-sized microelectrode arrays. Circuits created using photolithography are typically two dimensional, which restricted the design flexibility. Researchers have come up with innovative ways to fabricate 3D circuits using fabrication techniques meant for 2D patterning such as laser cutting (Figure 3) (91). There are also other fabrication techniques that allow the creation of soft deformable circuits on complex 3D curvilinear surfaces such as transfer printing techniques such as water transfer printing and stamp printing. In a typical transfer printing process, the conductive circuits are first prepared on a planar donor substrate and are then transferred to the target receiving substrate. This technique enables the creation of 2D circuits or electrodes on curved or 3D surfaces but is not able to create multilayer 3D circuits or electrodes. Zhang et al. reviewed various manufacturing techniques for the creation of soft deformable sensors on curved surfaces (92). In contrast, 3D printing is an additive manufacturing method whereby the electrode materials are additively deposited to the substrate according to the electrode designs. This enables the creation of multi-layered and multi-materials 3D circuits (93).

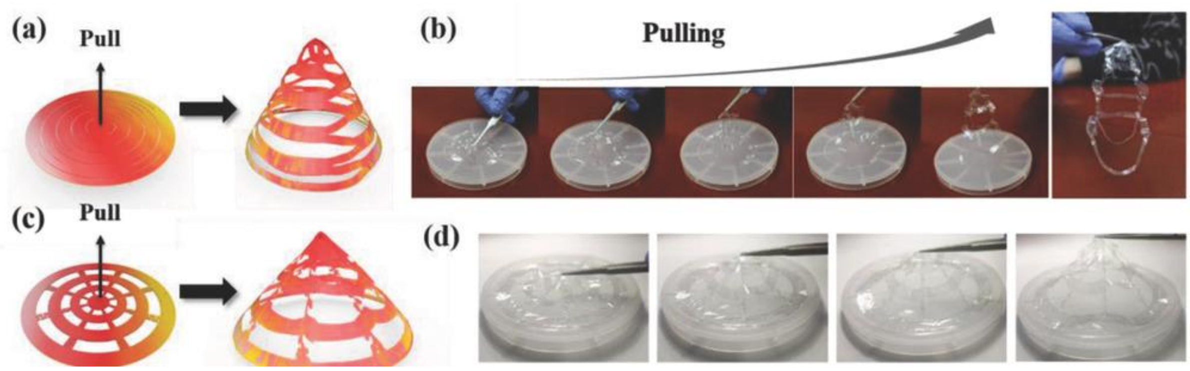


*Figure 3 a–d) Illustration and pictures taken during pulling processes demonstrating two examples of patterning hybrid film in a 2D plane and then being pulled into a 3D structure. Reproduced from (91) under the Creative Commons Attribution 4.0 International License.*

In contrast to electrodes for electrical stimulation and EEG purposes that usually require only a simple conducting structure, other types of sensors usually require more complicated designs such as multilayer architecture or multimaterial architecture. For instance, some resistive-based sensors such as pH sensor and pressure sensor have a pH- or pressure-sensitive sensing element and two connecting conductors that are usually made up of a different material from the sensing element (94, 95). Also, organic field-effect transistor (OFET)-based sensors that are usually made up of p-type and n-type semiconductors and arranged in a specific configuration can be used for various types of bioelectronic sensing purposes such as temperature, pressure, humidity, and chemical compounds (96). For instance, Lee et al. demonstrated using the use of field effect transistor with a single film of supported lipid bilayer to realize highly sensitive molecular detection in ionic environment as depicted in Figure 4 (97). Apart from conventional lithography manufacturing, these sensors can be easily fabricated using conventional printing techniques or 3D printing techniques (93). Other than electrodes and sensors, the use of electrochemical devices in bioelectronics is also very promising for sensing and energy storage applications (98, 99). For electrochemical sensors, they can usually come in a two-electrode or a three-electrode configuration. Depending on the sensing targets, the electrochemical electrodes can be selectively chosen to enhance the sensitivity of the measurement. On the other hand, for electrochemical storage devices such as supercapacitor and battery, they are usually fabricated through hydrothermal synthesis, electrochemical deposition, chemical vapor deposition, or physical methods such as coating, sputtering, and 3D printing (99). In order to achieve physical flexibility for bioelectronic devices, the materials used are usually conductive and flexible such as graphene, sheath-core yarn, carbon nanotubes, boron-carbon nanosheets, etc (99).

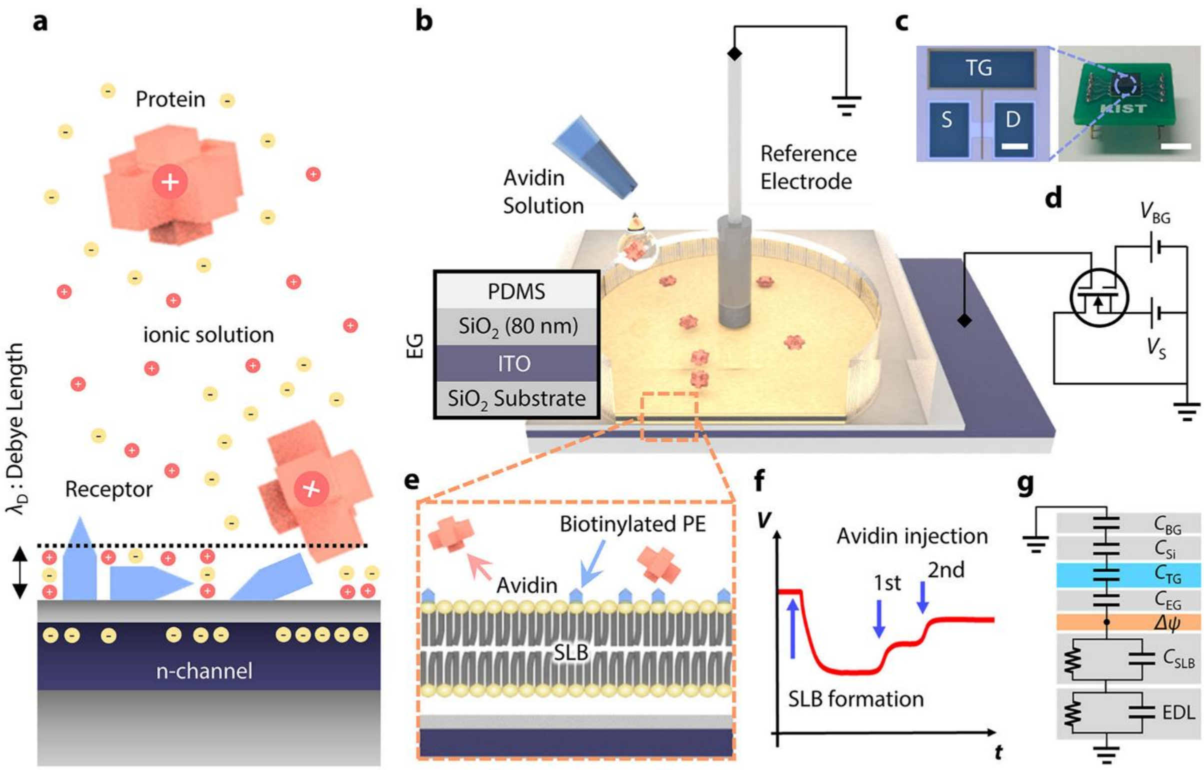


*Figure 4 Challenges to potentiometric measurement schemes for molecular detection on an FET under ionic environment: formation of the EDL, non-specific binding, and randomly oriented receptors. b Schematic representation of a reaction*

*chamber on the EG. (left) Layer-by-layer configuration of the EG. Polydimethylsiloxane (PDMS) chamber acts as a reaction chamber. c Optical images of the FET (left) and a packaged device (right) (scale bars = 100 µm and 5 mm, respectively). d Schematic representation of measurement setup. e Cross-sectional illustration of the SLB on the EG surface. f Proof-of-concept for real-time detection during biotin–avidin binding. g Equivalent circuit model for the measurement setup. Reproduced from (97) under the Creative Commons Attribution 4.0 International License.*

Bioprinting, a computer-assisted technology, deposits cell-based materials with spatial control over material deposition. As described by Guillemot et. al., is "the use of computer-aided transfer process for patterning and assembling living and non-living materials with a prescribed 2D or 3D organization" (100). This technology is closely related to its counterpart – additive manufacturing (AM) also known as 3D printing (101-103). A distinction from bioprinting's predecessor technology is to incorporate cells as the ink (i.e. bioink) in the printing process. As such, bioprinting technologies are divided into four main categories  material jetting, material extrusion, vat polymerization, and freeform spatial printing (also referred to as pick-and-place technologies) (104).

**Material Jetting (**Figure 5**i)** involves droplet displacement of material using technologies such as piezoelectric/thermal inkjetting, acoustic wave jetting, electrohydrodynamic jetting and laser induced forward transfer (105-111). As a crossover between material jetting and material extrusion, microvalve technology integrated at the nozzle regulates material flow which creates droplets or filaments based on the opening and closing of valve (112). **Material Extrusion (**Figure 5**ii)**techniques is a nozzle-based dispensing method that extrude bioink in a continuous manner (113-126). **Vat Polymerization Printing** (VPP) (**Figure 5iii**) fabricates construct through selectively curing a container filled with cell-hydrogel suspension using either laser in stereolithography (SLA) or area-projection in digital light processing (DLP) (127, 128). **Free-form spatial printing** (**Figure 5iv)** describe technologies that move cell units (be it single cell or cell clusters such as spheroids) in a spatially defined manner. These assembly technologies involves picking, either using magnetic field to lift magnetically labelled cell units (129, 130) or using laser to optically manipulate material from one substrate to another in laser guided direct writing (LGDW) (131) or vacuum aspiration to manipulate cell units in three dimensional spaces (132, 133).

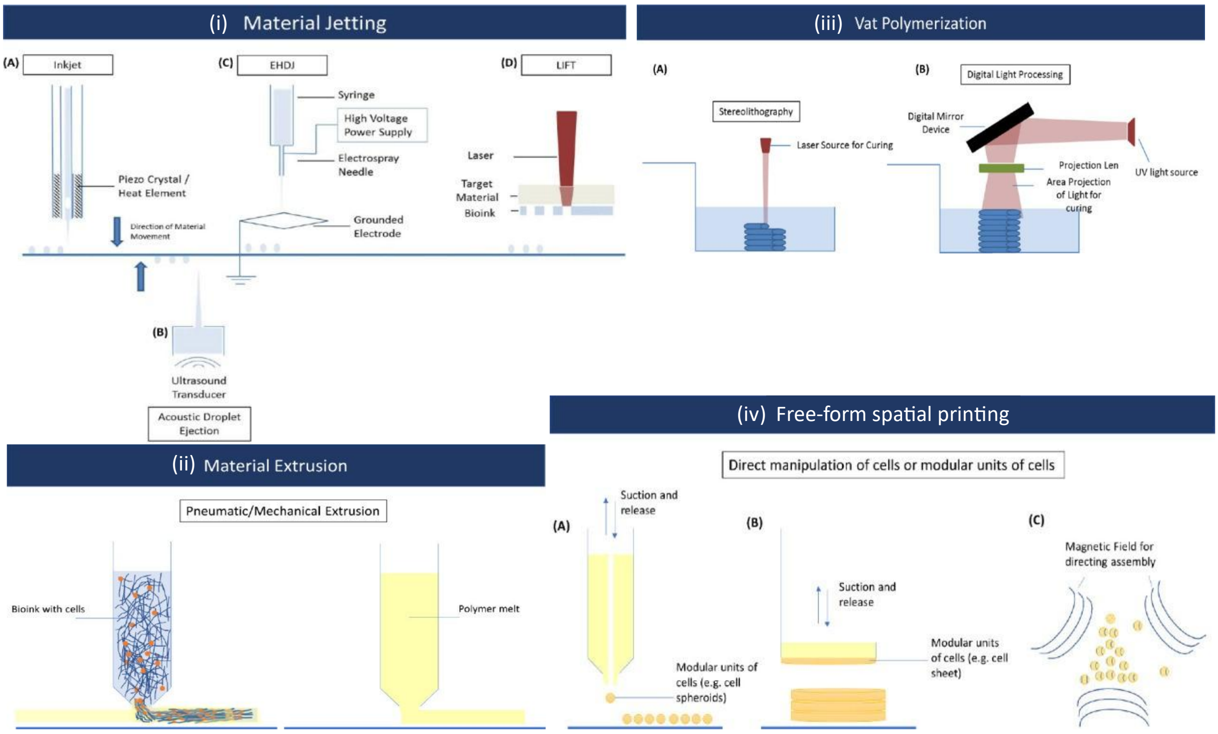


*Figure 5 Schematic showing different (i) material jetting, (ii) material extrusion, (iii) vat polymerization, and (iv) free-form spatial printing techniques. Reproduced from (134) under the Creative Commons Attribution 4.0 International License.*

3D printing is a very effective way to produce freestanding micropillar electrode arrays. Other than the microneedle electrode designs, 3D electrodes can also be achieved combining the rigid and brittle metal materials that are flat with a pre-stretched elastomeric substrate to form wavy, kirigami structures and mesh structures with an additional out-of-plane dimension.

In a nutshell, the research involving electrode design and manufacturing of electrodes for bioelectronics have been shifting towards improving the spatial resolution of the electrodes (135), enhancing the interfacial adhesion for lowering the skin/electrode impedance (136), and reducing the artefacts due to motions (137). Besides, researchers are also looking at customizing the electrode microstructure and configuration to increase the signal-to-noise ratio and spatial resolution (138, 139). Interestingly, machine learning techniques have also been used for developing customized model for improving the reconstruction accuracy and temporal resolution (140).

*3.3 Closed-loop system*

In bioelectronics, closed loop systems enable the communication between the living cells and artificial elements. A typical closed-loop system consists of sensors and stimulator, hardware, and software (Figure 6). Sensors pick up biological signal and convert it into electrical signal. An example of sensors would be the extracellular electrode, which can acquire biological signal without piercing the cell membrane through capacitive coupling. Typically, conversion of biological signal to electrical signal can be separated into: (i) Extracellular Action Potentials (EAP); (ii) Local Field Potentials (LFP); (iii) Electrode-Electrolyte Interface Potential (EEIP); and Stimuli Artifact (SA) (141-146). EAP commonly exist within the frequency range from 0.1 kHz to 10 kHz, whereas LFP exist between 1 Hz to 100 Hz (141). Both EAP and LFP provide useful activity info in the biological signal. EEIP originates from the potential difference between the electrode and electrolyte. The magnitude of the potential is electrode and time dependent (142). For instance, a gold electrode in a saline solution can have a EEIP of 50 mV (143). To put things into perspective, the EAP and LFP signal are typically in the range of 100 micro V and 1 mV. SA is a biological signal as result of the external stimulation. A typical stimulating voltage is around 1 V (144). Once the biological cell is stimulated, EEIP will take some time (in the order of milliseconds) to disperse the accumulated charge. As both the SA and EEIP exist in the same frequency band as the EAP and LFP, the information from EAP and FLP might be lost (145, 146). Hence, careful design consideration will be needed, which includes signal filtering and amplifying of the biological signal.

Acquisition hardware is a bridge between each individual sensor and stimulator and the software. Advanced acquisition hardware supports multichannel, which enables the development of multi electrodes arrays for multisite acquisition and stimulation (147). The acquisition hardware also filters and amplify the electrical signal from the electrodes and converts the analogy signal into digital signal which can be fed into the software. The hardware also transforms the digital signal from the software into the analog electrical signal to the stimulators.

The software analyses the acquired signal from the sensors to determine the state that the biological cells are in based on the patterns retrieved from the raw neural data, which include spikes, bursts, and stimulus artifacts. Conventional way of extracting patterns is rather manual and greatly relies on condition descriptors. The patterns can be extracted from the spike counts in a specific interval, as well as statistical techniques commonly used in neurophysiology such as the inter-burst interval histogram, inter-spike interval histogram, and post-stimulus-time histogram (147). The biological cells are said to be in a certain state if the patterns extracted from the sensors meet a set of conditions for that particular event. The feature extraction and condition-based algorithm is tedious and time-consuming and relies greatly on the experience of the users.

Successful deployment of the instantaneous closed-loop control approach is challenging due to the complexity of the human physiology. Interactions among the nervous, circulatory, and gastro-intestinal systems (all having non-linear dynamics) makes it difficult to estimate the state, not to mention controlling it for therapeutic benefit (148).

Due to the complexity of the human physiology, various types of sensors and stimulators would be required at different parts of the body in order for the closed-loop control system to work. This warrants the need to create a distributed network of bioelectronics sensors and acutators. The biological signal that can be measured by the biosensors include biochemical (eg. glucose, pH), thermal, mechanical (eg. strain, pressure) and electrical signals (ECG, EEG). These signals are critical in determining the physiological states. On the other hand, the biostimulator must be able to control physiological processes such as the neural activity, organ function, or biomolecule production.

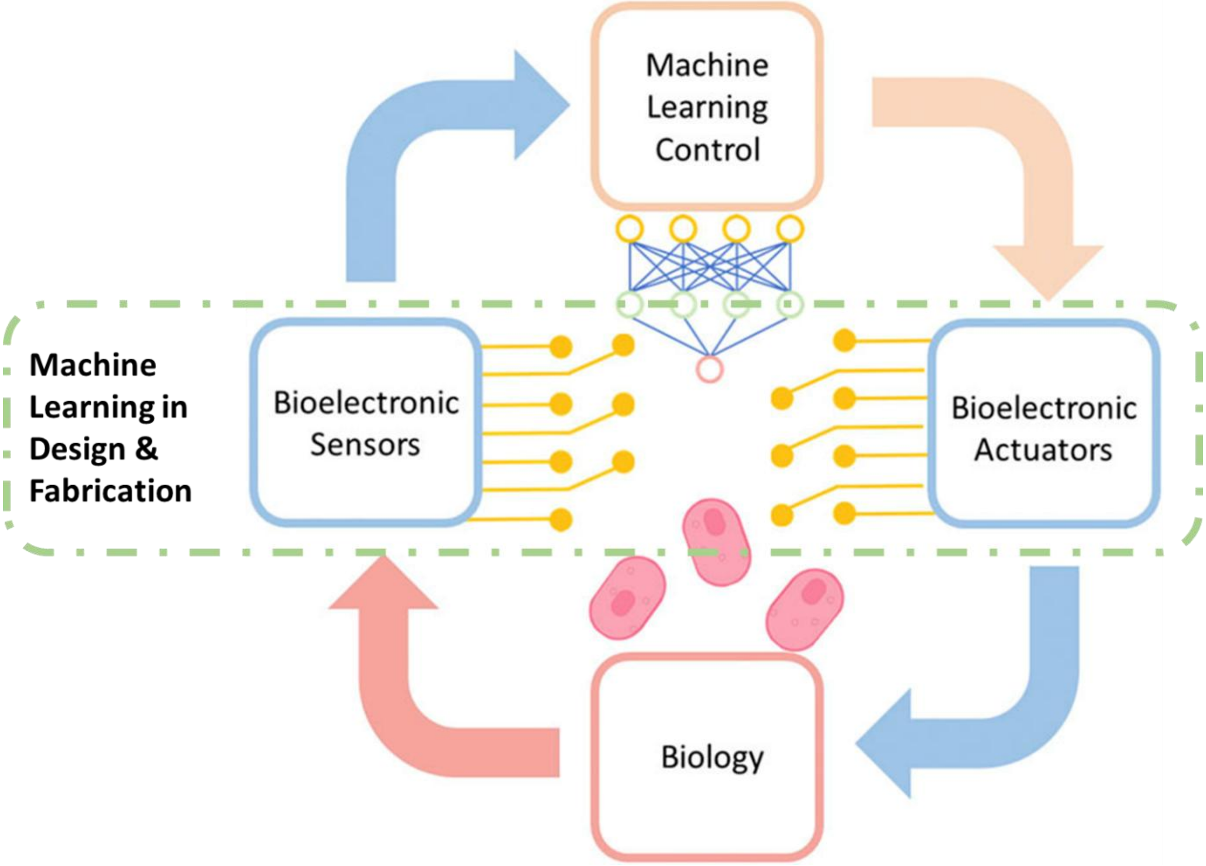


*Figure 6 A closed-loop bioelectronic system with the ML-control of bioelectronic actuators using sensor feedback. Adapted with permission from (149) . Copyright 2020, AIP Publishing.*

## 4. ML for Materials, Process, System in Bioelectronics

### *4.1 ML for Product development*

Bioelectronics rely greatly on the use of sensors to acquire useful data from the biological bodies. More often that not, multiple types of sensors will be used to monitor the biological activities. Moreover, the energy source and the wireless transmission of signal are two critical aspects to consider in the design of bioelectronics. The integration of multiple sensors and other component such as battery or wireless telemetry into a single platform reduces the footprint of the sensors. However, this would involve a huge amount of effort in the product design optimization stage, in terms of the sensing performance, dimensions of each component, battery life and wireless transmission range.

Apart from that, process optimization also needs to be done at the fabrication stage to ensure that the fabricated parts work as intended, at the same time to maximize the throughput of the fabrication process. Optimizing the fabrication process involves tuning of several process parameters. The process parameters could be dependent on each other and have interaction, resulting in multidimensional relationship that are hard to interpret and optimize. Machine Learning techniques are used to identify the relationship between the input process parameters and the resulting output of interest.

For instance, machine learning for bioprinting process development has been increasing, with the hope to increase efficiency in utilizing resources through balancing both virtual and physical experiments. While at its infancy, objectives for using ML in bioprinting are distinct which is to identify process parameters efficient in printing engineered tissue (i.e. printability of material and process optimization) and to identify the biological functionality of the printed construct (i.e. prediction of cell viability) (150). ML has also been applied to perform in-situ correction to ensure consistency in print quality (151).

ML for bioprinting has mainly focused on process optimization. Deploying machine learning algorithms to enhance dimensional accuracy. For instance, Ruberu et al. used Bayesian optimization (BO) technique to quantitatively evaluate the printability of gelatin methacryloyl (GelMA) and hyaluronic acid methacrylate (HAMA) bioinks and to perform optimization to achieve the manufacturing of reproducible 3D scaffold with minimum experimentation (Figure 7) (152). The BO is able to find global optima with significant smaller sample size compared to other optimization methods such as genetic algorithms. In the study, BO was used to minimize the print score, which takes into account of the layer stacking quality and the filament morphology quality. The technique narrows down the number of optimal print settings to as low as 4 from 6,000-10,000 possible print settings to identify the optimal print setting, accelerating the tedious and time-consuming optimization process.

In material jetting technique for bioprinting, it is noted that improved the print precision can be achieved by using a nozzle diameter, and bio-inks with lower viscosity and surface tension but at the expense of greater amount of satellite formation. Shi et al developed a hybrid multi-subgradient descent bundle method with an adaptive learning rate algorithm (HMSGDBA), which utilizes the multi-subgradient descent bundle (MSGDB) method with Adam algorithm to look for the optimal print parameters and material properties that can print with high precision and stability for the fabrication of cell arrays (153). Computational Fluid Dynamic (CFD) simulation was used to study the piezoelectric inkjet printing process and the satellite formation. A fully-connected neural network was created to acquire the relationship between the process and material parameters such as the voltage, viscosity, surface tension, and nozzle diameter and the satellite formation, which defines the quality of the deposited droplet. The HMSGDBA was able to get a set of print parameters that is close to the global optimum and successfully improved the print precision and stability. Wu et al. have done similar work to predict the droplet formation of the inkjet based bioprinting process (154). In the work, ensemble learning algorithm that incorporates random forest (RF), least absolute shrinkage and selection operator (LASSO), scalable machine learning system for tree boosting (XGBoost), and support vector regression (SVR) was applied to acquire the relationship between the process parameters such as the polymer concentration, excitation voltage, dwell time, and rise time and the droplet formation characteristics such as the droplet velocity and volume.

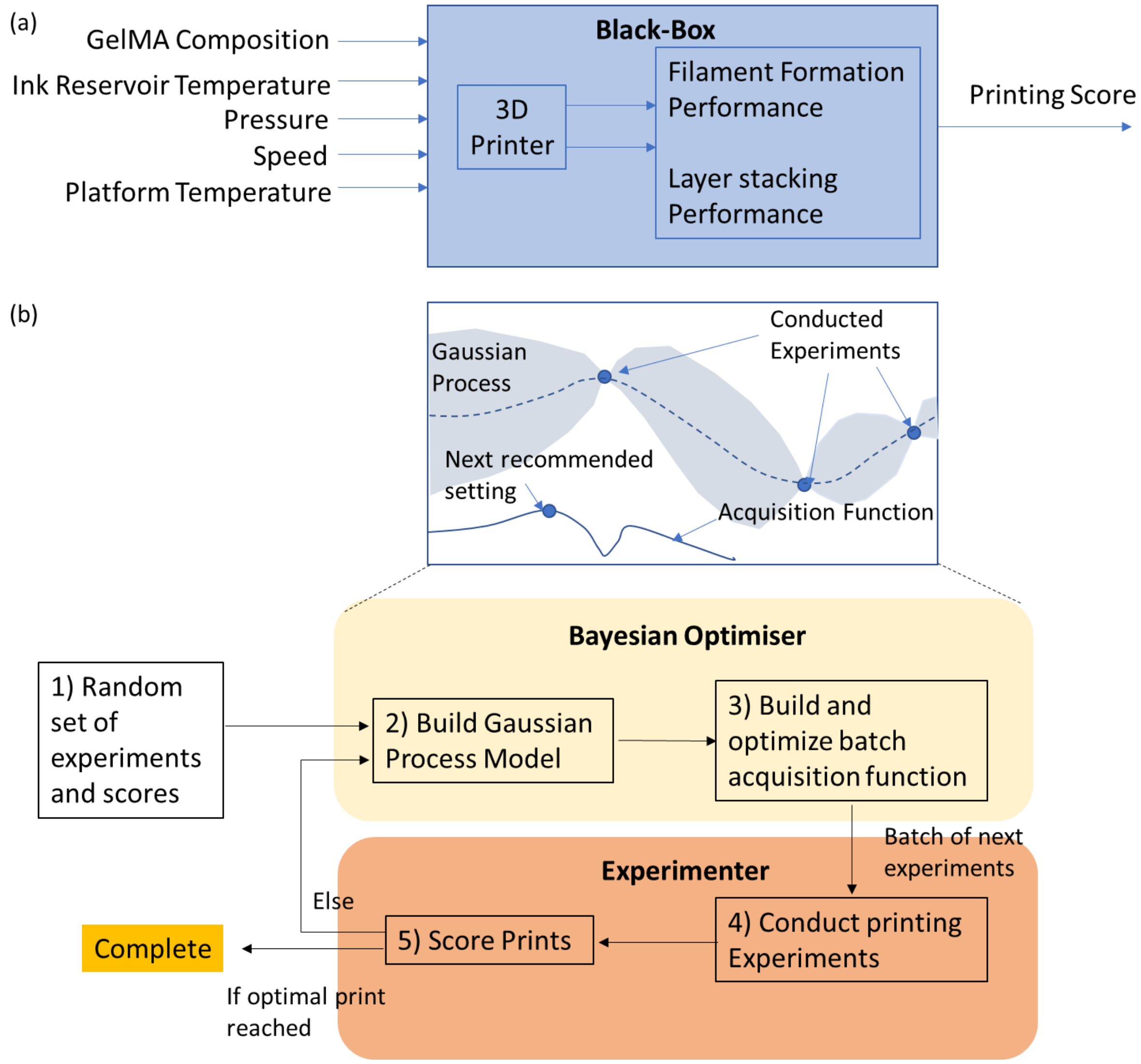


*Figure 7 a) System to be optimized b) Bayesian Optimisation framework (152).*

Guan used ML to identify process parameters that accounts for scattering effects induced by cells in the DLP process (155). Cells in the bioink induces a strong scattering effect which arises from the refractive index mismatch between cytoplasm and hydrogel. Firstly, trial data was acquired from a variety of sample masks with various smooth and sharp features. The printed structures were imaged using a fluorescence microscope to obtain binary image of 0 and 1 representing voids and polymerized area respectively. The processed image and its affiliated mask were used to train the algorithm. Guan and team continued to generate various virtual data as output using the input data obtained previously. The result is a simulator that was calibrated and subsequently used to train the neural network (NN). NN-calculated masks were found to compensate for scattering effect by protruding sharp regions while shrinking into denting regions. These augmenting functions help preserve features of complex structures in DLP.

In SLA for bioprinting, UV irradiation is known to damage deoxyribonucleic acid (DNA) of the cell through the formation of cyclobutene pyrimidine dimer. There are various and complicated routes of cell damage which complicates the physics-based model for good cell viability prediction. Xu et al. used an ensemble learning algorithm, that contains and outperforms the base learners such as the ridge regression (RR), k-nearest neighbors (KNN), random forest (RF), and NN, to predict the cell viability of the SLA-printed biomaterial based on process parameters such as the UV intensity, exposure time, layer thickness, and material concentration with a $R^2$ of 0.953 (156).

Aerosol jet printing has been widely used to fabricate advanced electronics with fine resolution and complicated geometry, due to its ability to perform conformal printing and to process a broad range of materials. In aerosol jet, the active conductive material are usually bounded with a layer of organic stabilizer which makes them not conductive. Intense pulsed light is one of the sintering process used to remove the organic stabilizer and fuse the active materials. Goh et al. found that there is a contradiction relationship between the sintering parameters and the film thickness on the electrical performances of the aerosol-jet printed conductive ink (157). To obtain an optimum set of process parameters, the group used ML to perform multi-objective optimization between two contradicting features. They used a technique that combines the use of a central composite design (CCD), a response surface methodology, a desirability function, and a non-dominated sorting genetic algorithm III. The data-driven technique created on the basis of statistical modelling, analysis of variance and global optimization was able to reduce the contradiction between the design and post processing parameters, resulting in a crack-free printed lines with low resistivity. Similar approach has also been used by Zhang et al. to optimize the printed line quality of the Aerosol jet printed conductive traces (158).

Reproducibility has always been an important factor in any manufacturing process. In tissue engineering, it is crucial to preserving the biocompatibility and structural integrity required for engineered tissue constructs. Jin et al. developed a layer-by-layer image monitoring technique to predict imperfections within the printed bio constructs (Figure 8)(159). A convolutional neural network (ResNeXt-50) to detect various anomalies, infill pattern and location information with an average accuracy of 90%. Similar work has been done by Jin et al. (160)

and Goh et al. (161) to detect anomalies (underextrusion and overextrusion) in material extrusion process.

Through the use of the ML classification algorithm, Nadernezhad determines that a formulation with high yield viscosity and a low degree of plasticity prior to flow, whereas the transition from Newtonian to non-Newtonian behaviour of the flow occurs at relatively low shear rates is deemed printable in extrusion bioprinting (162). As such, features such as yield viscosity, ratio of storage modulus at flow point to the limit of viscoelastic range, and the consistency index of the Carreau-Yasuda model are important guidelines suggested by the author in designing new formulations.

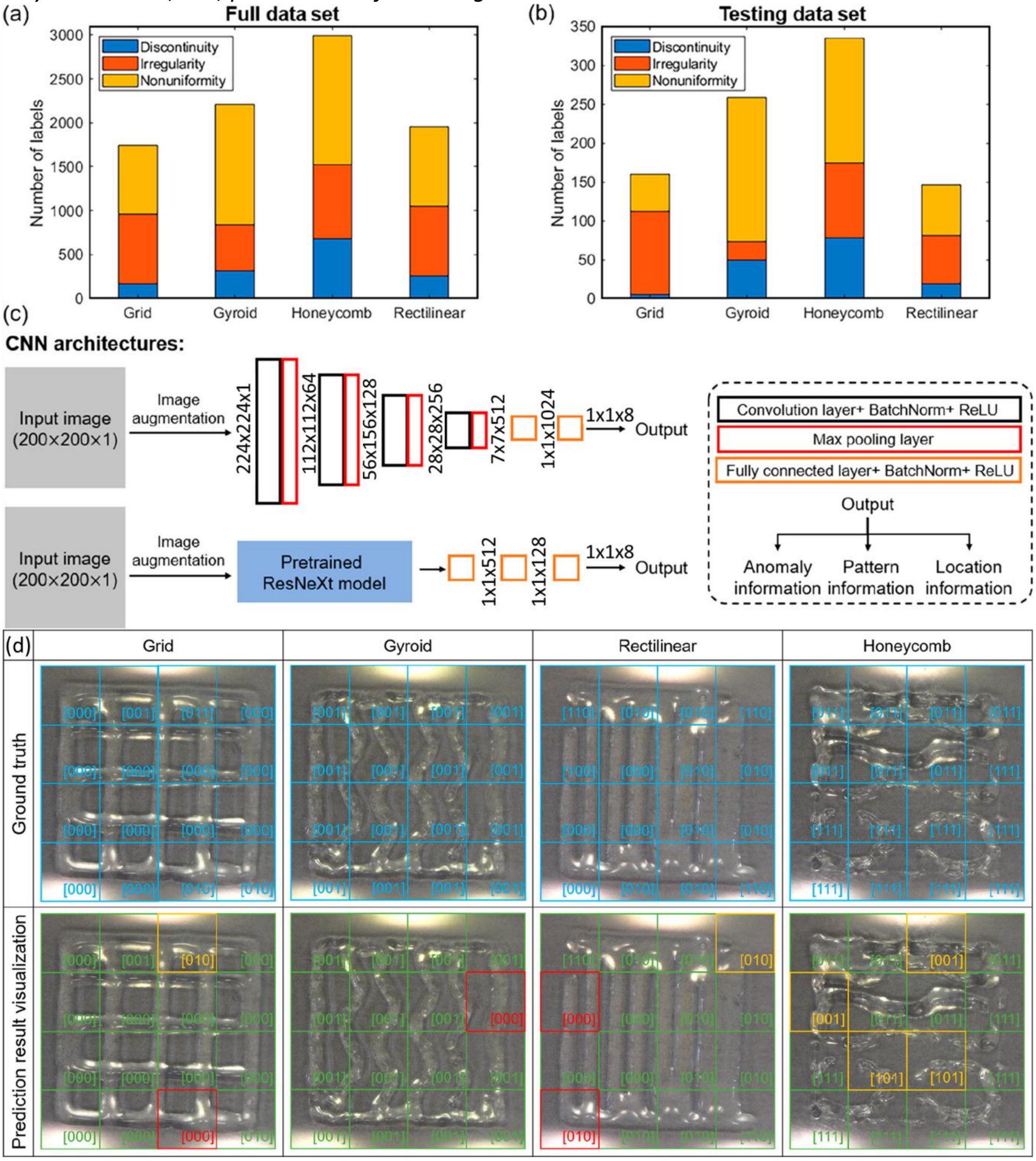


*Figure 8 (a,b) Bar charts showing anomaly information for both full and testing data sets. The number of labels for three types of anomalies under four infill patterns is shown. (c) Flow diagram showing the architectures of applied CNN models. The self-designed CNN architecture is illustrated at the top, and the pretrained model is shown at the bottom. (d) Anomaly detection result visualization on test data. Adapted with permission from (159). Copyright 2021, American Chemical Society.*

Table 5 summarizes the research works on the use of ML for the fabrication processes.

*This is the accepted version of the following article: Machine Learning for Bioelectronics on Wearable and Implantable Devices: Challenges and Potential, which has now been formally published in final form at Tissue Engineering Part A at https://doi.org/10.1089/ten.tea.2022.011. This original submission version of the article may be used for non-commercial purposes in accordance with the Mary Ann Liebert, Inc., publishers' self-archiving terms and conditions.*

*Table 5 Summary of the use of ML for the fabrication processes.*

| Fabrication processes | Materials | Inputs | Outputs | ML techniques | Unique features | Refs. |
|---|---|---|---|---|---|---|
| Material Extrusion | • gelatin methacryloyl (GelMA)<br>• hyaluronic acid methacrylate (HAMA) bioinks | • GelMA composition<br>• Ink Reservoir Temperature<br>• Pressure<br>• Speed<br>• Platform Temperature | • Print Quality (printing score) | Bayesian Optimisation | Significantly reduces the number of experimentations | (152) |
| Material Jetting | • HeLa cells<br>• Dulbecco's Modified Eagle Medium (DMEM)<br>• sodium alginate (SA) dissolved in DMEM | • Voltage<br>• Viscosity<br>• Surface tension<br>• Nozzle diameter | • Droplet formation | hybrid multi-subgradient descent bundle method with an adaptive learning rate algorithm (HMSGDBA | Multi-objective optimization Simulation data is used | (153) |
| Material Jetting | • sodium alginate hydrogel<br>• NIH/3T3 mouse fibroblast | • Voltage<br>• Rise Time<br>• Dwell time<br>• Polymer concentration | • Droplet velocity location<br>• Ejected volume | ensemble learning algorithm that combines RFs, LASSO, XGBoost, and SVR | | (154) |
| Stereolithography | • GelMA and Lithium phenyl-2,4,6-trimethylbenzoylphosphinate (LAP) | • UV intensity<br>• UV exposure time<br>• gelatin methacrylate concentration<br>• and layer thickness | • cell viability | Ensemble learning algorithm combining neural networks, ridge regression, K-nearest neighbors, and random forest (RF) | real-time monitoring and accurate prediction of cell viability under varying printing conditions | (156) |

| | | | | | | |
|---|---|---|---|---|---|---|
| Material Extrusion | | • 200 × 200 pixels square image | • Anomaly information<br>• Grid infill pattern<br>• Location information | • Support vector machine (SVM) model is trained on the histogram of oriented gradients (HoG)<br>• ResNeXt-50 (CNN) | Anomaly detection of printed patterns | (159) |

*4.2 ML for sensing and actuation*

ML techniques are useful when there are no accurate mathematical model to describe the biological responses. ML techniques learn from a large amount of data to draw inference on the complex non-linear relationship between input and output and are can be used to close the loop for bioelectronic systems comprising biosensors and bioelectronic actuators.

For instance, the instantaneous control of the pH in solution using machine learning has been showcased by a few research groups (163-165). This technique can be broadened to modulate the cell membrane voltage ($V_{mem}$) through regulating the pH with an addition of control hierarchy. The hierarchy consists of three stages: a decision maker, a planner, and a low-level controller. The decision maker regulates the temporary goals (pH values) that, consequently, influence the long-haul goals ($V_{mem}$). The planner facilitates the actions needed by the decision maker and the low-level controller that communicates with the bioelectronic sensors and stimulators. For instance, the planner provide the relationship between $V_{mem}$ and the change in pH that is required by the decision maker, and regulating the control points smooth operation of bioelectronics stimulators. The ML-based controller comprises a radial basis function (RBF) artificial neural network, which consists an input layer, a hidden layer, and an output layer (Figure 9). The input layer takes in targeted responses and the measured responses at different instants. The hidden layer maps out the required $V_{H^+}$ to achieve the targeted [$H^+$]. The benefit of using ML for the closed-loop control is that it is robust to uncertainties and non-linearities due to electric field-induced temporal ionic currents and the membrane bound ion channel activity.

ML learning techniques have been applied in the design of the implantable closed-loop solutions. For instance, a few algorithms have been created in the past decades for seizure detection (166-169). Most of the algorithms used the time-domain feature and pattern recognition. Spatiotemporal relationship is used to predict seizure. Apart from that, frequency-based approaches have been used by extracting spectral information from the EEG signals. This approach would require preprocessing of data and extraction of the best feature to be input to SVM model for classification (170).

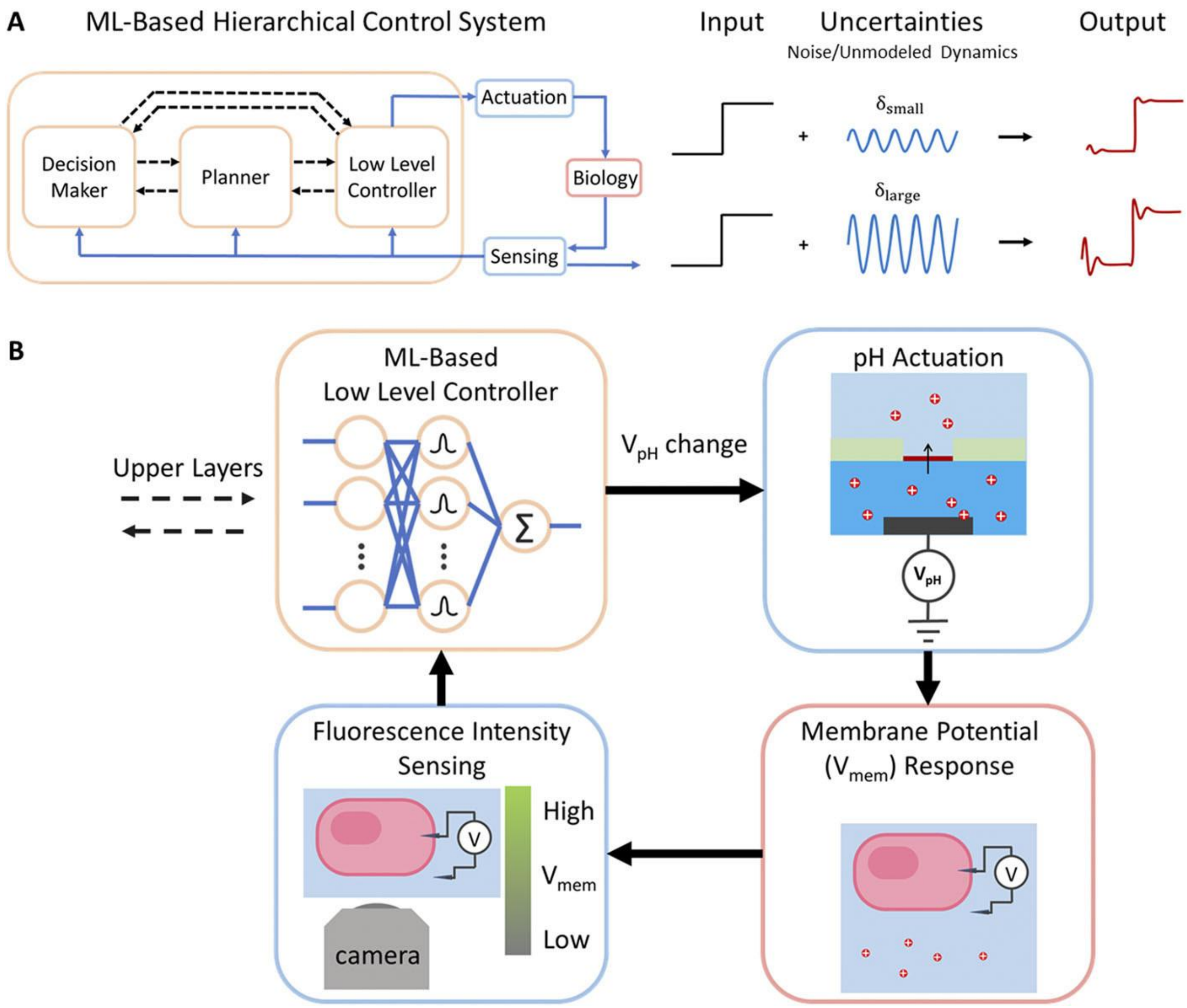


*Figure 9 (a) The multi-level control system and its main components (i.e., the decision-maker, planner, and low-level controller) and its robustness to uncertainties, noise, and unmodeled dynamics. (b) Machine learning-based system for $V_{mem}$ control using pH modifying bioelectronics and fluorescence feedback. Adapted with permission from (149) . Copyright 2020, AIP Publishing.*

Machine learning techniques have been used to perform calibration of sensors, especially those that exhibit significant non-linearity. For instance, the carbon nanotube field-effect transistors have been shown to exhibit ultra-low detection limits (in the range of parts-per-billion concentration). However, they are prone to signal saturation at higher concentrations, making conventional statistical model such as linear regression model not effective in predicting at higher concentration. Bian et al. used regression trees and random forest to model the response of the sensors at different concentrations (171). Using the ML techniques, they have successfully improved the $R^2$ to 0.826 using out-of-bag error and increased the dynamic range of the sensors up to 12 orders of magnitude in concentration.

Zhang and Tao used ANN with 24 hidden layers to classify human activities based on 12 features extracted from the ECG, Electrooculography (EOG), electro-bacterial-graph (EBG), and electromyography (EMG) signals (172). The chemi- and electro-physiological signals were obtained from the GEPC-based transient epidermal electronics, which can provide comprehensive physiological states of the humans. The ANN was able to achieve an classification accuracy of 96.9% based on the multidimensional physiological signatures obtained from the sensors.

In an attempt to develop a strain-isolated, wearable soft bioelectronic system, Rodeheaver et al. used residual CNN model, with 5 convolutional layers and 4 deconvolutional layers, to classify human activities (idle, walk, fast walk, jogging) based on data retrieved from accelerometers (173). It is reported that an overall accuracy of 99.3% was achieved. Coupled with breathable soft membrane integrated with ECG electronic system for heart rate and respiratory rate data, the wearable bioelectronics can be used to monitor health continuously and wirelessly up to 8 hrs, making it suitable for consumer and clinical settings.

ML techniques have also been used to detect hand gestures via the EMG) signals. For instance, Kwon et al. used residual CNN and KNN to classify various hand gestures through the EMG signals picked up from the nanomembrane containing functionalized conductive graphene (Figure 10) (174). The EMG devices were positioned on several muscles, such as the almaris longus, brachioradialis, and flexor carpi ulnaris. Average root-mean-square value was calculated from the EMG signal and used as the inputs for the ML models to learn to classify the various hand gesture. The group highlighted that a training time of merely 140 s is required to train the ML model as only a small dataset is required. The same group has also applied the same technique to determine the leg postures (175).

*This is the accepted version of the following article: Machine Learning for Bioelectronics on Wearable and Implantable Devices: Challenges and Potential, which has now been formally published in final form at Tissue Engineering Part A at [https://doi.org/10.1089/ten.tea.2022.011](https://doi.org/10.1089/ten.tea.2022.011). This original submission version of the article may be used for non-commercial purposes in accordance with the Mary Ann Liebert, Inc., publishers' self-archiving terms and conditions.*

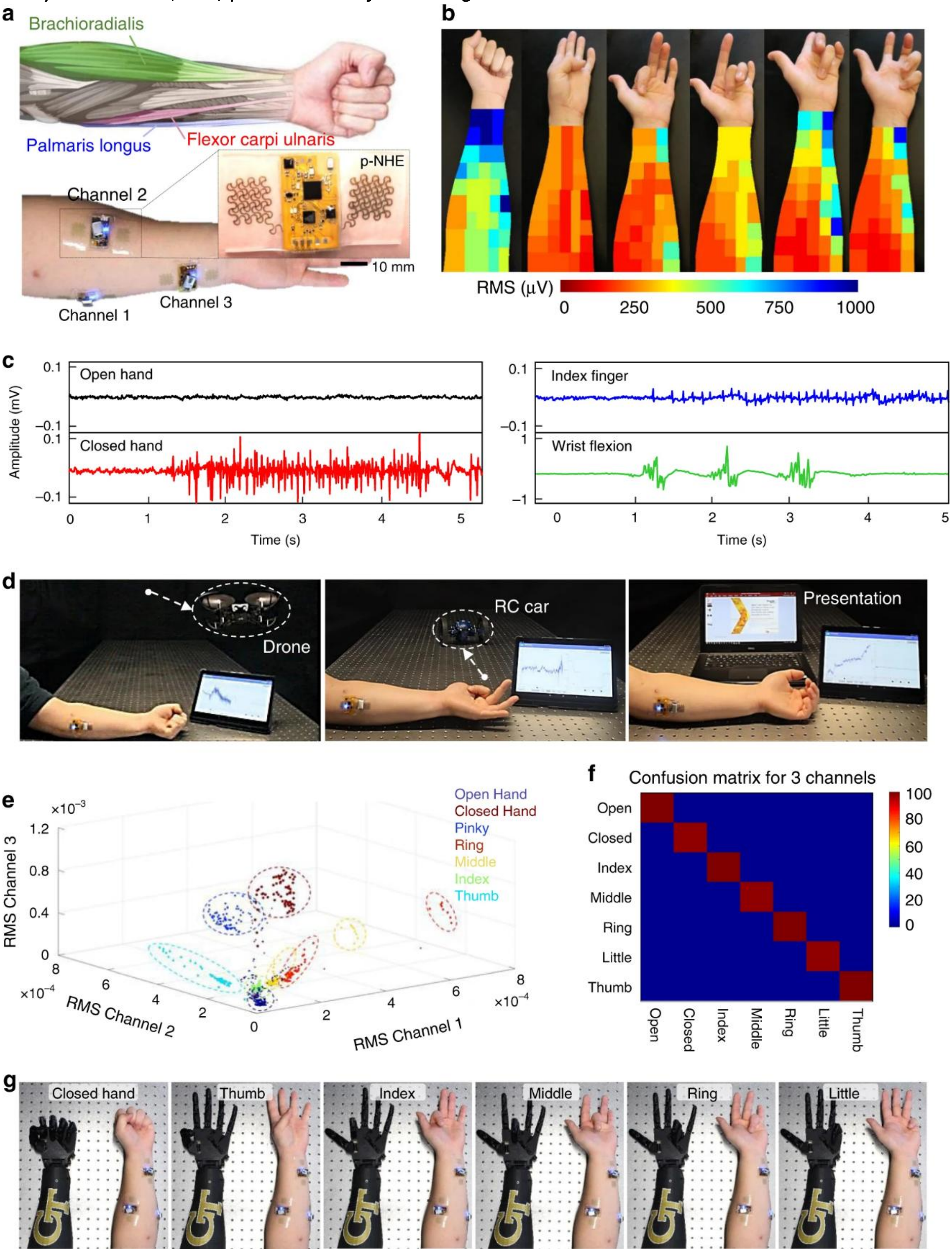


*Figure 10 a) Drawing illustrating specific muscles on forearm to detect various hand postures and photos capturing three p-NHE placed on specific muscles, including palmaris longus, brachioradialis, and flexor carpi ulnaris. B) EMG mapping data illustrating RMS signals from multiple channels that encompasses the whole forearm; six different heat maps are generated based on six gestures. C) Representative EMG signals from four gestures, including open hand, closed hand and index finger flexion and wrist flexion. D) Demo of EMG-enabled human-machine interfaces with a wireless, wearable p-NHE to precisely* *control a flying drone, RC car, and presentation software. E) 3D plot of three-channel, EMG RMS signals for clear differentiation of seven different gestures as seven groups. F) Result of real-time, confusion matrix from ten trials, showing 98.6% accuracy across seven classes with three-channel EMG recording. G) Demo of a three-channel EMG recording and corresponding control of a robotic hand, demonstrating examples of six motions of a subject and following motions of the robotic hand. Reprinted with permission from (174). Copyright 2020, Nature.*

The design space for the biosenors can be large due to multiple design parameters involved, making it hard to obtain a suitable set of design parameters for the most optimum sensing performance. Machine learning techniques have also been applied in the design of sensors for improved performance more easily. For instance, to design meta-plasmonic biosensors, Moon et al. used autoencoder and t-Stochastic Neighbor Embedding (t-SNE) to cluster optical characteristic of meta-plasmonic structure by reducing the dimension of the dataset, and used k-means clustering to group the angular reflectance curves (176). Using the technique, the optimum parameter sets can be obtained without using much computational resources and allows for a more systematic understanding of feature effects.

Chen et al. compared the performance of the generic random forest classifier and the weighted-average classifiers for the development of ultrasonic-based sensor for monitoring respiratory behaviours (Figure 11) (177). The ultrasonic sensors measures the non-linear change in local circumference of the chest and abdominal walls during the respiration process, which is also affected by the postures. Various features, including the first-order differential, second order differential, wavelet decomposition, and mean value with variance, are extracted from the ultrasonic signals. Using the random forest technique, it was found that the wavelet decomposition is the most important feature, showing high significance in both time and frequency domains for retrieving useful respiratory features for classifier training. It was found that generic classifier gives low accuracy in estimating the posture of the subjects, whereas the weighted-adaptive classifier gives higher accuracy making it suitable for custom-tailored individual model for precision medicine.

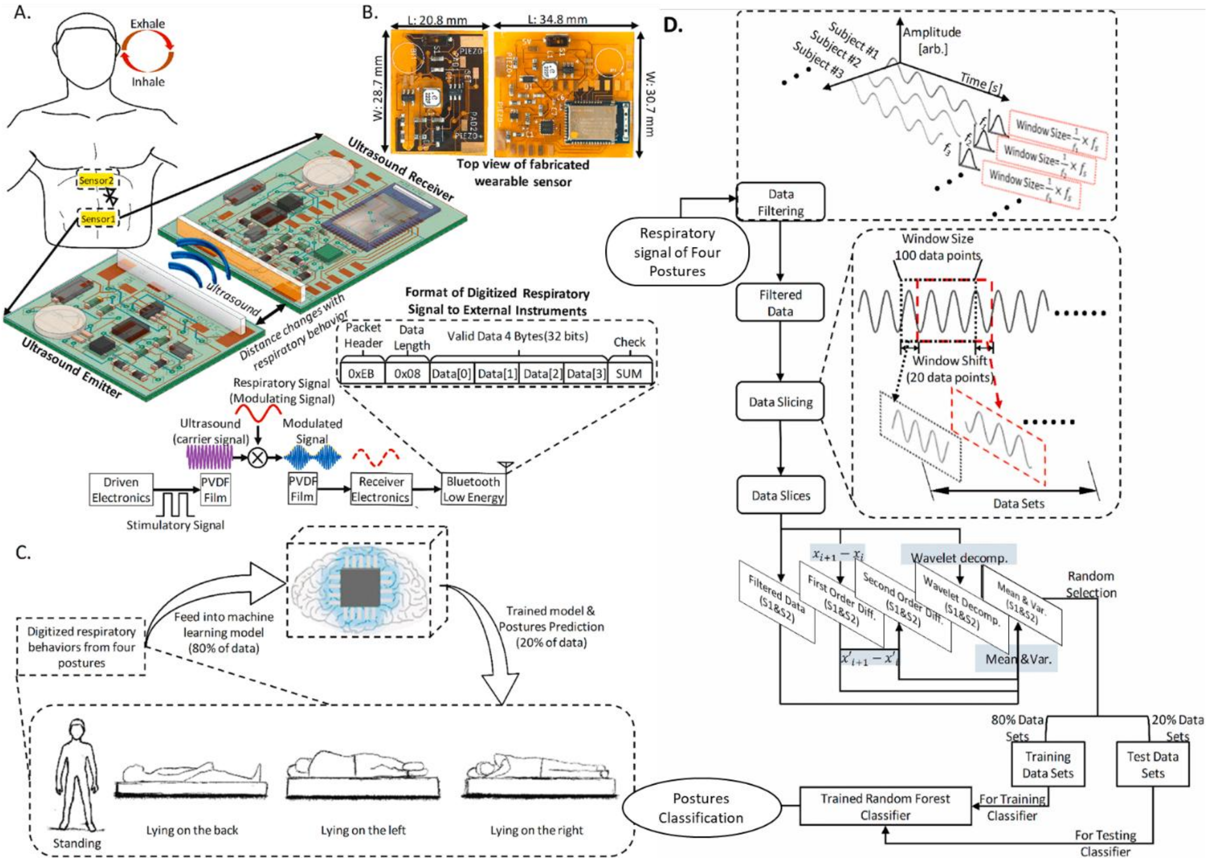


*Figure 11 (A) Wireless wearable sensors positioned on the midway of the xiphoid process and the costal margin, one on each location, corresponding to the abdomen-apposed rib cage, and 1 cm above the umbilicus, respectively.(B) Picture of the fabricated wireless wearable sensor on a flexible polyimide substrate. (C) Respiratory behaviors data obtained from four postures of subjects were input to a ML algorithm. (D) ML algorithm process flow.*

Mahmood et al. developed a nanomembrane sensors to detect blepharospasm (178). EMG signals picked up from the sensor is split into 8 second segments and processed with a 0.2 Hz high-pass filter before feeding into the CNN. Semantic segmentation was used due to it ability to pinpoint the precise duration of the symptoms. The CNN technique enables efficient training on small datasets with high accuracies, and is able to classify normal blinking, futter blinking, blepharospasm, and hemifacial spasm with an average accuracy of 99.1 ± 2.8%.

Mahmood et al. developed a bioelectronic systems capable of performing VR text spelling and navigation via 4 EEG signals (179). Using CNN and 4-fold cross-validation, the highest achievable accuracy for detecting 33 classes was around 78.93% from 0.8 s of data. It was found that longer time length of data provide higher accuracy (91.73% for 2 s).

An et al. used compared the performance of the machine learning techniques with the non-machine learning method (traditional thresholding method) in the development of the triboelectric nanogenerator network for neck motion detection (Figure 12) (180). It was found that the trained CNN model was able to detect 11 classes of neck movement with an average accuracy of 92.63%, which is significantly higher compared to that of the traditional thresholding method that achieved 77.17%. It was also noted that the traditional thresholding method was not able to achieve high detection accuracy with small rotation (3°). The CNN model, on the other hand, was able to achieve 86.68%, by training it with 2 sessions of data with rotation and 4 sessions of data without rotation.

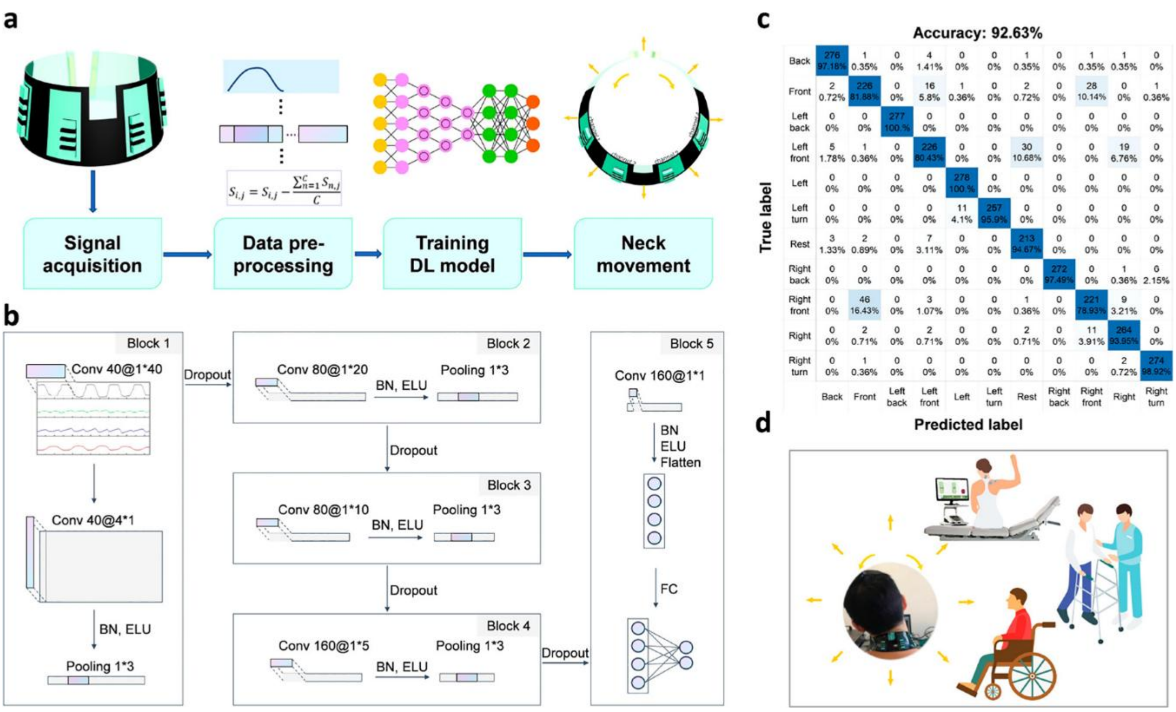


*Figure 12 Neck movement state identification system with integrated DL-aided data analytics. (a) Overall structure and data flow of the neck movement identification system. (b) Detailed structure of the CNN training model. (c) Confusion matrix of recognizing 11 different neck movement states, showing a high accuracy of 92.63%. (d) Applications of the neck movement identification system in healthcare, rehabilitation, machine control, etc. Reproduced with permissions from (180) ,Copyright © 2022, American Chemical Society*

Kim et al. developed an electronic skin that detects dynamic motions through a single signal channel without the use of large sensor network (Figure 13). A long short-term memory (LSTM) network was used to recognize the hand motions through identifying the corresponding temporal behaviours of the signal from the sensor. The trained model is able to achieve an accuracy of 92.9%. They also used transfer learning techniques to apply the existing knowledge on the sensor behaviours to the new users. By doing so, only a small amount of training sample is required from the new users and the retraining of the model

*This is the accepted version of the following article: Machine Learning for Bioelectronics on Wearable and Implantable Devices: Challenges and Potential, which has now been formally published in final form at Tissue Engineering Part A at [https://doi.org/10.1089/ten.tea.2022.011](https://doi.org/10.1089/ten.tea.2022.011). This original submission version of the article may be used for non-commercial purposes in accordance with the Mary Ann Liebert, Inc., publishers' self-archiving terms and conditions.*

using the newly collected data just took around 5 mins. In comparison, without using the transfer learning, it would take around 20 mins to achieve the same performance as the one trained with transfer learning.

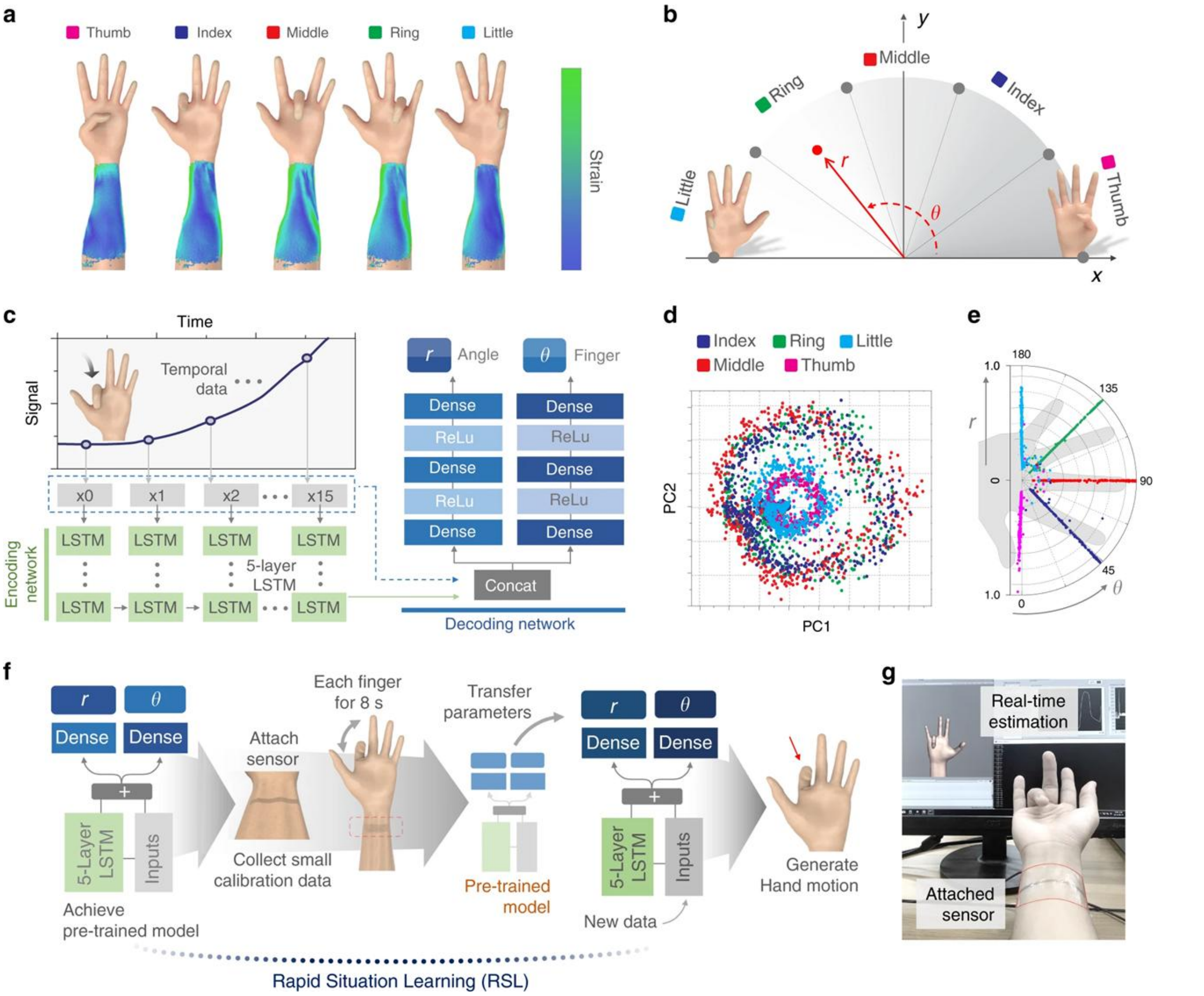


*Figure 13 a Illustration of skin deformations for various finger bending motions. b Metric space defining single finger bending motions: physical alignment of fingers in a hand is expressed in the metric space with R representing the amount of a finger bent and ϑ identifying the position of a finger in a hand. c Neural network consisting an encoding network and a decoding network. LSTM layers are used in encoding network to analyze temporal sensor patterns to generate latent vectors. Two independent dense layers map created latent vectors to our metric space expressing hand motions. Dropout is used as the regularization technique to prevent the network to be overfitted to a single use case. d 2D PCA illustration of output vectors produced by encoding network. Each circular cluster shows that encoding network can precisely recognise cyclic finger motions from sequential sensor inputs. e Figure of how sensor inputs in training dataset are mapped to the metric space after passing our network. f The processes of rapid situation learning (RSL) that utilizes transfer learning. When the sensor is attached to a new position and a small amount of retraining data is collected, the new network utilizes knowledge learned during pretraining by transferring parameters from pretrained network, reducing the amount of dataset, and time for retraining. g Photo of actual hand motion generation. Reproduced from (181) under the Creative Commons Attribution 4.0 International License.*

Halilaj et al. reviewed the use of machine learning in human movement biomechanics and discussed the best practices and common drawbacks in applying the machine learning techniques in biomechanics (182). In the review, various applications that integrated sensors and machine learning techniques to track movement pattern to monitor certain diseases automatically on a daily basis in the out-of-clinic settings. Some of the best practices have also been also proposed to avoid some common pitfalls when applying machine learning techniques. Interested readers are encouraged to refer to the full manuscript to learn more about it.

Table 6 summarizes the research works on the use of ML for the development of bioelectronics.

*Table 6 Summary of the use of ML in the sensing and actuation of bioelectronics*

| Purpose | Input | output | ML techniques | Unique features | Refs. |
|---|---|---|---|---|---|
| Regulate pH | desired values at time k + 1, k, and k − 1, measured values at time k − 1, k − 2, and k − 3 | $V_{H^+}$ | RFB-ANN | • No assumption needed<br>• Robust to variability | (163, 164) |
| Sensor calibration | 6 features including (conductance change at different potential difference, relative transconductance, threshold voltage change) | Mercury ions concentration | • Regression Tree<br>• Random Forest<br>• Out of Bag error | overcome ssaturation and widens the dynamic range of the nanosensors up to 12 orders of magnitude in analyte concentrations | (171) |
| Motion Artifact-Controlled Health monitoring | • acceleration data | • Idle<br>• walk<br>• fast walk<br>• jog | • CNN | detect types of activities, as well as, exact time spent performing each category | (173) |
| Human-machine interactions | • EMG signals<br>• Accelerations data | • Seven types of hand gestures | • 2-layer CNN model<br>• KNN | • Using hand gesture to control drone<br>• 99% accuracy | (174, 175) |
| Pyshiological mononitoring | • 3 features from ECG<br>• 3 features from EMG<br>• 3 features from EOG | • 4 Physcio-logical states (vigorous, exercising, | • ANN with 24 hidden layers | • 96.9% accuracy<br>• transient epidermal electronic | (172) |

| | | | | | |
|---|---|---|---|---|---|
| | • 3 features from EBG | tired, stimulated) | | array could simultaneously provide electro- and chemo-physiological signal | |
| To design meta-plasmonic biosensors. | | | • multilayer perceptron (MLP) and autoencoder (AE)<br>• t-SNE<br>• k-means clustering | Achieved improved detection sensitivity | (176) |
| Posture classification | Respiratory signals from ultrasonic sensors (filtered signals, first order differential, second-order differential, mean values with variances, wavelet decomposition) | 4 postures ( standing, lying on the back, lying of the left, and lying on the right) | • random forest classifier | Weighted adaptive classifiers performs better than generic classifier | (177) |
| To diagnose Blepharospasm | electrophysiological signals | Four activities (null, blink, force spasm, and hemifacial spasm) | • CNN semantic segmentation | achieved an accuracy of 99.1 ± 2.8% | (178) |
| VR text spelling and navigation | Four 1s segment EEG signals | 33 classes | • Spatial-CNN | accuracy of 78.93% for 0.8 s and 91.73% for 2 s with 33 classes from nine human subjects | (179) |
| To detect neck motion | 4 Triboelectric signals around the neck | 11 neck motions | • CNN | accuracy of 92.63% | (180) |
| To decode the complex motion of five fingers | Resistive sensors with laser-induced crack | Finger bending motions | • Long short-term memory (LSTM) | • Accuracy of 96.2%<br>• Transfer learning | (181) |

| | | | | | |
|---|---|---|---|---|---|
| | | | | shortens the retraining time from 20 to 5 mins | |

## 5. Summary and Perspective

The use of ML in bioelectronics covers different aspects, ranging from material formulation, design and fabrication to data acquisition and control of actuators. ML has been shown in several occasions to be an effective tool in the process optimization and classification the physiological states through the data acquired from the sensors. Nonetheless, we could foresee the increasing ML research efforts on close-loop system for bioelectronics, which includes the control of the bio actuators, which would continue to push the knowledge boundary of smart bioelectronics in years to come. We also anticipate that more sophisticated ML algorithms will be developed to further improve the computational speed and performance.

Despite the advantages, there exists several challenges in applying ML in the design, fabrication, and sensing and actuation of the bioelectronics. An important concern is related to the possible inaccuracy of the ML's predictions due to data mismatch between the training and actual environment. When inferring data that falls outside of the range of the training data, ML algorithms that relies on past trained data may erroneously give a wrong prediction, which is unacceptable especially for critical health applications. This can be circumvented using robust, big data-driven and transferable ML algorithms to reduce any possible errors. It is well known that one of the major challenges about applying ML techniques in any real-life application is the availability of the dataset for training the ML algorithms, especially for different environments, ages, and genders. This would require expertise in both computer science, biology, and medicine to perform data labelling and feature extraction to create high-quality dataset for training. Fortunately, some emerging algorithms, such as the few-shot learning that only need small datasets, creates the possibility to address the challenge. Meta-learning is another ML algorithm that learn to adapt to unfamiliar environments with minimum number of samples (183). Another way to solve the challenge on small datasets is by performing data augmentation and transfer learning, where the ML model is originally trained on a similar and data-abundant task then finetuned on the main task (184).

Another challenge is the computational cost, which plays a critical role in close-loop control. Bioelectronics are typically small to ensure they are easy to wear and install. Electronics components, including the CPU are miniaturized at the expense of processing performance. This makes it a challenge for the miniaturized processors to handle ML tasks, such as CNN, which require high computational power. Nonetheless, much effort has been paid on the development of small ML models with good prediction accuracy. The advances in the silicone chip industry to come up with smaller sized processing unit with higher computational power would aid in the development of smart bioelectronics.

Deep learning models have been thought as black boxes that are difficult to explain the underlying relationship of the data. This may bring about mistrust from relevant stakeholders like the medical practitioners and regulators. Making ML models explainable without giving up performance is a heavily investigated field. In image classification and object detection, for instance, interpretability techniques can pinpoint pixels that have the most significant contribution to the model's prediction. For bioprinting and sensor-printing tasks that require input parameters, there are some ML approaches that are able to explain which printing parameters will have the most significant effect to the prediction by perturbing the input parameters. Such interpretability tools will garner confidence from relevant stakeholders as ML-enabled fabrication of sensors continues to progress.

The review is focused on highlighting the feasibility of applying state-of-the-art ML techniques into various research fields in the development of bioelectronics. We envision that the development of smart bioelectronics would likely come to pass through the use of ML-enabled material formulation, design, fabrication, sensing and actuation. For instance, machine learning techniques will continue to aid in the discovery of novel materials with tailored properties for bioelectronics, such as the transient electronics. The use of machine learning together with large datasets containing the fabrication process parameters and the material properties speeds up the design process by allowing designers to virtually simulate the performance of the bioelectronics and have multiple design iterations without having to fabricate them physically, saving time and material. Nonetheless, bioelectronics typically relies more on than one sensor to determine the state of the body. The use of multiple sensors poses challenges on the data management and the processing speed of computer, especially so for those portable bioelectronics, such as the health monitoring devices, that usually have CPUs with low computing power. More advanced machine learning techniques that can achieve high accuracy and fast detection rate would be required before daily health monitoring in the out-of-clinic settings can be realized. Also, although machine learning techniques have been applied in bioelectronics to create closed-loop systems and have shown promising results, the data collected were mainly from controlled-lab environment, leading to poorer-than-expected performance in actual usage. More tests are required to validate their performance under the normal daily usage.

**CRediT author statement**

**Guo Dong Goh**: Conceptualization, writing - Original draft preparation, Writing - Review & Editing.

**Jia Min Lee**: Conceptualization, writing - Original draft preparation

**Guo Liang Goh**: writing - Original draft preparation

**Xi Huang**: writing - Original draft preparation

**Samuel Lee**: writing - Original draft preparation

**Wai Yee Yeong**: Project administration, Supervision, Funding acquisition

**Acknowledgment**

The authors acknowledge the support of National Research Foundation for NRF Investigatorship Award No.: NRF-NRFI07-2021-0007.

The research is supported by the National Research Foundation, Prime Minister's Office, Singapore under its Medium-Sized Centre funding scheme.

**Authors disclosure statement**

The authors declare no conflict of interest.

**References**

1. Ouyang H, Liu Z, Li N, et al. Symbiotic cardiac pacemaker. Nature Communications. 2019;10(1):1821; doi:10.1038/s41467-019-09851-1.

2. Lee S, Wang H, Shi Q, et al. Development of battery-free neural interface and modulated control of tibialis anterior muscle via common peroneal nerve based on triboelectric nanogenerators (TENGs). Nano Energy. 2017;33:1-11; doi:10.1016/j.nanoen.2016.12.038.
3. Long Y, Li J, Yang F, et al. Wearable and Implantable Electroceuticals for Therapeutic Electrostimulations. Advanced Science. 2021;8(8):2004023; doi:10.1002/advs.202004023.
4. Sunwoo SH, Ha KH, Lee S, et al. Wearable and Implantable Soft Bioelectronics: Device Designs and Material Strategies. In: Doherty MF, Segalman RA, editors. Annual Review of Chemical and Biomolecular Engineering, Vol 12, 2021. Annual Review of Chemical and Biomolecular Engineering. 122021. p. 359-91.
5. Zhou HL, Zhang Y, Qiu Y, et al. Stretchable piezoelectric energy harvesters and self-powered sensors for wearable and implantable devices. Biosensors & Bioelectronics. 2020;168; doi:10.1016/j.bios.2020.112569.
6. Lee G-H, Moon H, Kim H, et al. Multifunctional materials for implantable and wearable photonic healthcare devices. Nature Reviews Materials. 2020;5(2):149-65; doi:10.1038/s41578-019-0167-3.
7. Chen X, Villa NS, Zhuang Y, et al. Stretchable Supercapacitors as Emergent Energy Storage Units for Health Monitoring Bioelectronics. Advanced Energy Materials. 2020;10(4):1902769; doi:10.1002/aenm.201902769.
8. Jiang DJ, Shi BJ, Ouyang H, et al. Emerging Implantable Energy Harvesters and Self-Powered Implantable Medical Electronics. Acs Nano. 2020;14(6):6436-48; doi:10.1021/acsnano.9b08268.
9. Fanelli A, Ferlauto L, Zollinger EG, et al. Transient Neurovascular Interface for Minimally Invasive Neural Recording and Stimulation. Advanced Materials Technologies. 2022;7(2):2100176; doi:10.1002/admt.202100176.
10. Ko G-J, Han SD, Kim J-K, et al. Biodegradable, flexible silicon nanomembrane-based NOx gas sensor system with record-high performance for transient environmental monitors and medical implants. NPG Asia Materials. 2020;12(1):71; doi:10.1038/s41427-020-00253-0.
11. Koo J, MacEwan MR, Kang S-K, et al. Wireless bioresorbable electronic system enables sustained nonpharmacological neuroregenerative therapy. Nature Medicine. 2018;24(12):1830-6; doi:10.1038/s41591-018-0196-2.
12. Kim D-H, Viventi J, Amsden JJ, et al. Dissolvable films of silk fibroin for ultrathin conformal bio-integrated electronics. Nature materials. 2010;9(6):511-7;
13. Moreno S, Keshtkar J, Rodriguez-Davila RA, et al. Bioelectronics on Mammalian Collagen. Advanced Electronic Materials. 2020;6(8):2000391; doi:10.1002/aelm.202000391.
14. Liu LX, Liang HY, Zhang J, et al. Poly(vinyl alcohol)/Chitosan composites: Physically transient materials for sustainable and transient bioelectronics. Journal of Cleaner Production. 2018;195:786-95; doi:10.1016/j.jclepro.2018.05.216.
15. Zheng Q, Zou Y, Zhang Y, et al. Biodegradable triboelectric nanogenerator as a life-time designed implantable power source. Science Advances. 2016;2(3):e1501478; doi:doi:10.1126/sciadv.1501478.
16. Zhang Y, Zhou Z, Fan Z, et al. Self-Powered Multifunctional Transient Bioelectronics. Small. 2018;14(35):1802050; doi:10.1002/smll.201802050.
17. Lei T, Guan M, Liu J, et al. Biocompatible and totally disintegrable semiconducting polymer for ultrathin and ultralightweight transient electronics. Proceedings of the National Academy of Sciences. 2017;114(20):5107-12; doi:doi:10.1073/pnas.1701478114.
18. Feng S, Tian Z, Wang J, et al. Laser Sintering of Zn Microparticles and Its Application in Printable Biodegradable Electronics. Advanced Electronic Materials. 2019;5(3):1800693; doi:10.1002/aelm.201800693.
19. Fu KK, Wang Z, Dai J, et al. Transient Electronics: Materials and Devices. Chemistry of Materials. 2016;28(11):3527-39; doi:10.1021/acs.chemmater.5b04931.

20. Han WB, Lee JH, Shin JW, et al. Advanced Materials and Systems for Biodegradable, Transient Electronics. Advanced Materials. 2020;32(51); doi:10.1002/adma.202002211.
21. Feig VR, Tran H, Bao ZN. Biodegradable Polymeric Materials in Degradable Electronic Devices. Acs Central Science. 2018;4(3):337-48; doi:10.1021/acscentsci.7b00595.
22. Li CM, Guo CC, Fitzpatrick V, et al. Design of biodegradable, implantable devices towards clinical translation. Nature Reviews Materials. 2020;5(1):61-81; doi:10.1038/s41578-019-0150-z.
23. Yu X, Shou W, Mahajan BK, et al. Materials, Processes, and Facile Manufacturing for Bioresorbable Electronics: A Review. Advanced Materials. 2018;30(28):1707624; doi:10.1002/adma.201707624.
24. Singh R, Bathaei MJ, Istif E, et al. A Review of Bioresorbable Implantable Medical Devices: Materials, Fabrication, and Implementation. Advanced Healthcare Materials. 2020;9(18):2000790; doi:10.1002/adhm.202000790.
25. Caruana R, Niculescu-Mizil A. An Empirical Comparison of Supervised Learning Algorithms. Icml '06. 2006:161–8; doi:10.1145/1143844.1143865.
26. Ghahramani Z. Unsupervised Learning. In: Bousquet O, von Luxburg U, Rätsch G, editors. Advanced Lectures on Machine Learning: ML Summer Schools 2003, Canberra, Australia, February 2 - 14, 2003, Tübingen, Germany, August 4 - 16, 2003, Revised Lectures. Berlin, Heidelberg: Springer Berlin Heidelberg; 2004. p. 72-112.
27. Hastie T, Tibshirani R, Friedman J. Unsupervised Learning. In: Hastie T, Tibshirani R, Friedman J, editors. The Elements of Statistical Learning: Data Mining, Inference, and Prediction. New York, NY: Springer New York; 2009. p. 485-585.
28. Arulkumaran K, Deisenroth MP, Brundage M, et al. Deep Reinforcement Learning: A Brief Survey. IEEE Signal Processing Magazine. 2017;34(6):26-38; doi:10.1109/MSP.2017.2743240.
29. Wiering MA, Van Otterlo M. Reinforcement learning. Adaptation, learning, and optimization. 2012;12(3):729;
30. Kaelbling LP, Littman ML, Moore AW. Reinforcement learning: A survey. Journal of artificial intelligence research. 1996;4:237-85;
31. Cortes C, Vapnik V. Support-vector networks. Machine Learning. 1995;20(3):273-97; doi:10.1007/BF00994018.
32. Quinlan JR. Simplifying decision trees. International Journal of Man-Machine Studies. 1987;27(3):221-34; doi:10.1016/S0020-7373(87)80053-6.
33. Breiman L. Random Forests. Machine Learning. 2001;45(1):5-32; doi:10.1023/A:1010933404324.
34. Wang S-C. Artificial neural network. Interdisciplinary computing in java programming: Springer; 2003. p. 81-100.
35. Abiodun OI, Jantan A, Omolara AE, et al. State-of-the-art in artificial neural network applications: A survey. Heliyon. 2018;4(11):e00938; doi:10.1016/j.heliyon.2018.e00938.
36. Witten IH, Frank E, Hall MA, et al., editors. Practical machine learning tools and techniques. DATA MINING; 2005.
37. Rojas R. AdaBoost and the super bowl of classifiers a tutorial introduction to adaptive boosting. Freie University, Berlin, Tech Rep. 2009;
38. Bauer E, Kohavi R. An Empirical Comparison of Voting Classification Algorithms: Bagging, Boosting, and Variants. Machine Learning. 1999;36(1):105-39; doi:10.1023/A:1007515423169.
39. Ahmad A, Dey L. A k-mean clustering algorithm for mixed numeric and categorical data. Data & Knowledge Engineering. 2007;63(2):503-27; doi:10.1016/j.datak.2007.03.016.
40. Chen CW, Luo J, Parker KJ. Image segmentation via adaptive K-mean clustering and knowledge-based morphological operations with biomedical applications. IEEE Transactions on Image Processing. 1998;7(12):1673-83; doi:10.1109/83.730379.

41. Wold S, Esbensen K, Geladi P. Principal component analysis. Chemometrics and Intelligent Laboratory Systems. 1987;2(1):37-52; doi:10.1016/0169-7439(87)80084-9.
42. Abdi H, Williams LJ. Principal component analysis. WIREs Computational Statistics. 2010;2(4):433-59; doi:10.1002/wics.101.
43. Bro R, Smilde AK. Principal component analysis. Analytical methods. 2014;6(9):2812-31;
44. Wall ME, Rechtsteiner A, Rocha LM. Singular Value Decomposition and Principal Component Analysis. In: Berrar DP, Dubitzky W, Granzow M, editors. A Practical Approach to Microarray Data Analysis. Boston, MA: Springer US; 2003. p. 91-109.
45. Silver D, Huang A, Maddison CJ, et al. Mastering the game of Go with deep neural networks and tree search. Nature. 2016;529(7587):484-9; doi:10.1038/nature16961.
46. Bellman R. A Markovian decision process. Journal of mathematics and mechanics. 1957:679-84;
47. Watkins CJCH, Dayan P. Q-learning. Machine Learning. 1992;8(3):279-92; doi:10.1007/BF00992698.
48. Lecun Y, Bottou L, Bengio Y, et al. Gradient-based learning applied to document recognition. Proceedings of the IEEE. 1998;86(11):2278-324; doi:10.1109/5.726791.
49. LeCun Y, Bengio Y, Hinton G. Deep learning. Nature. 2015;521(7553):436-44; doi:10.1038/nature14539.
50. Li Y, Chen Y, Wang N, et al., editors. Scale-aware trident networks for object detection. Proceedings of the IEEE/CVF International Conference on Computer Vision; 2019.
51. Tan M, Le Q, editors. Efficientnet: Rethinking model scaling for convolutional neural networks. International conference on machine learning; 2019: PMLR.
52. Karras T, Laine S, Aila T, editors. A style-based generator architecture for generative adversarial networks. Proceedings of the IEEE/CVF conference on computer vision and pattern recognition; 2019.
53. Amodei D, Ananthanarayanan S, Anubhai R, et al., editors. Deep speech 2: End-to-end speech recognition in english and mandarin. International conference on machine learning; 2016: PMLR.
54. Yu D, Deng L. Automatic speech recognition: Springer; 2016.
55. Young T, Hazarika D, Poria S, et al. Recent trends in deep learning based natural language processing. ieee Computational intelligenCe magazine. 2018;13(3):55-75;
56. Singh SP, Kumar A, Darbari H, et al., editors. Machine translation using deep learning: An overview. 2017 international conference on computer, communications and electronics (comptelix); 2017: IEEE.
57. Albawi S, Mohammed TA, Al-Zawi S, editors. Understanding of a convolutional neural network. 2017 International Conference on Engineering and Technology (ICET); 2017 21-23 Aug. 2017.
58. Schuster M, Paliwal KK. Bidirectional recurrent neural networks. IEEE Transactions on Signal Processing. 1997;45(11):2673-81; doi:10.1109/78.650093.
59. Harland B, Aqrawe Z, Vomero M, et al. A Subdural Bioelectronic Implant to Record Electrical Activity from the Spinal Cord in Freely Moving Rats. Advanced Science.n/a(n/a):2105913; doi:10.1002/advs.202105913.
60. Otchy TM, Michas C, Lee B, et al. Printable microscale interfaces for long-term peripheral nerve mapping and precision control. Nature Communications. 2020;11(1):4191; doi:10.1038/s41467-020-18032-4.
61. Song E, Li R, Jin X, et al. Ultrathin Trilayer Assemblies as Long-Lived Barriers against Water and Ion Penetration in Flexible Bioelectronic Systems. ACS Nano. 2018;12(10):10317-26; doi:10.1021/acsnano.8b05552.

62. Caravaca AS, Tsaava T, Goldman L, et al. A novel flexible cuff-like microelectrode for dual purpose, acute and chronic electrical interfacing with the mouse cervical vagus nerve. Journal of Neural Engineering. 2017;14(6):066005; doi:10.1088/1741-2552/aa7a42.
63. Moon H, Park B, Hong D, et al. 3D-structured soft bioelectronic devices with crack-free metal patterns. Sensors and Actuators B: Chemical. 2021;343:130123; doi:10.1016/j.snb.2021.130123.
64. Rowan CC, Graudejus O, Otchy TM. A Microclip Peripheral Nerve Interface (μcPNI) for Bioelectronic Interfacing with Small Nerves. Advanced Science. 2022;9(3):2102945; doi:10.1002/advs.202102945.
65. Yuk H, Lu B, Zhao X. Hydrogel bioelectronics. Chemical Society Reviews. 2019;48(6):1642-67; doi:10.1039/C8CS00595H.
66. Yang C, Suo Z. Hydrogel ionotronics. Nature Reviews Materials. 2018;3(6):125-42; doi:10.1038/s41578-018-0018-7.
67. Lang C, LaNasa JA, Utomo N, et al. Solvent-non-solvent rapid-injection for preparing nanostructured materials from micelles to hydrogels. Nat Commun. 2019;10(1):3855; doi:10.1038/s41467-019-11804-7.
68. Won D, Kim J, Choi J, et al. Digital selective transformation and patterning of highly conductive hydrogel bioelectronics by laser-induced phase separation. Science Advances. 2022;8(23); doi:10.1126/sciadv.abo3209.
69. Hong I, Lee S, Kim D, et al. Study on the oxidation of copper nanowire network electrodes for skin mountable flexible, stretchable and wearable electronics applications. Nanotechnology. 2019;30(7):074001; doi:10.1088/1361-6528/aaf35c.
70. Won P, Park JJ, Lee T, et al. Stretchable and Transparent Kirigami Conductor of Nanowire Percolation Network for Electronic Skin Applications. Nano Lett. 2019;19(9):6087-96; doi:10.1021/acs.nanolett.9b02014.
71. Kim D, Bang J, Won P, et al. Biocompatible Cost‐Effective Electrophysiological Monitoring with Oxidation‐Free Cu–Au Core–Shell Nanowire. Advanced Materials Technologies. 2020;5(12); doi:10.1002/admt.202000661.
72. Lee S, Sasaki D, Kim D, et al. Ultrasoft electronics to monitor dynamically pulsing cardiomyocytes. Nat Nanotechnol. 2019;14(2):156-60; doi:10.1038/s41565-018-0331-8.
73. Subraveti SN, Raghavan SR. A Simple Way to Synthesize a Protective "Skin" around Any Hydrogel. ACS Applied Materials & Interfaces. 2021;13(31):37645-54; doi:10.1021/acsami.1c09460.
74. Yang J, Bai R, Chen B, et al. Hydrogel Adhesion: A Supramolecular Synergy of Chemistry, Topology, and Mechanics. Advanced Functional Materials. 2020;30(2):1901693; doi:10.1002/adfm.201901693.
75. Li S, Cong Y, Fu J. Tissue adhesive hydrogel bioelectronics. Journal of Materials Chemistry B. 2021;9(22):4423-43; doi:10.1039/D1TB00523E.
76. Deng J, Yuk H, Wu J, et al. Electrical bioadhesive interface for bioelectronics. Nature Materials. 2021;20(2):229-36; doi:10.1038/s41563-020-00814-2.
77. Kai H, Yamauchi T, Ogawa Y, et al. Accelerated Wound Healing on Skin by Electrical Stimulation with a Bioelectric Plaster. Advanced Healthcare Materials. 2017;6(22):1700465; doi:10.1002/adhm.201700465.
78. Schiavone G, Lacour SP. Conformable bioelectronic interfaces: Mapping the road ahead. Science Translational Medicine. 2019;11(503):eaaw5858; doi:10.1126/scitranslmed.aaw5858.
79. Li G, Wang S, Duan YY. Towards conductive-gel-free electrodes: Understanding the wet electrode, semi-dry electrode and dry electrode-skin interface impedance using electrochemical impedance spectroscopy fitting. Sensors and Actuators B: Chemical. 2018;277:250-60; doi:10.1016/j.snb.2018.08.155.
80. Green RA, Baek S, Poole-Warren LA, et al. Conducting polymer-hydrogels for medical electrode applications. Science and Technology of Advanced Materials. 2010;11(1):014107;

81. Wang K, Parekh U, Pailla T, et al. Stretchable dry electrodes with concentric ring geometry for enhancing spatial resolution in electrophysiology. Advanced healthcare materials. 2017;6(19):1700552;
82. Huang D, Li J, Li T, et al. Recent advances on fabrication of microneedles on the flexible substrate. Journal of Micromechanics and Microengineering. 2021;
83. Srivastava AK, Bhartia B, Mukhopadhyay K, et al. Long term biopotential recording by body conformable photolithography fabricated low cost polymeric microneedle arrays. Sensors and Actuators A: Physical. 2015;236:164-72;
84. An K, Hong S, Han S, et al. Selective Sintering of Metal Nanoparticle Ink for Maskless Fabrication of an Electrode Micropattern Using a Spatially Modulated Laser Beam by a Digital Micromirror Device. ACS Applied Materials & Interfaces. 2014;6(4):2786-90; doi:10.1021/am405323c.
85. Pan H, Hwang DJ, Ko SH, et al. High-Throughput Near-Field Optical Nanoprocessing of Solution-Deposited Nanoparticles. Small. 2010;6(16):1812-21; doi:10.1002/smll.201000345.
86. Hong S, Lee H, Yeo J, et al. Digital selective laser methods for nanomaterials: From synthesis to processing. Nano Today. 2016;11(5):547-64; doi:10.1016/j.nantod.2016.08.007.
87. Park JH, Han S, Kim D, et al. Plasmonic-Tuned Flash Cu Nanowelding with Ultrafast Photochemical-Reducing and Interlocking on Flexible Plastics. Advanced Functional Materials. 2017;27(29):1701138; doi:10.1002/adfm.201701138.
88. Krieger KJ, Liegey J, Cahill EM, et al. Development and Evaluation of 3D-Printed Dry Microneedle Electrodes for Surface Electromyography. Advanced Materials Technologies. 2020;5(10):2000518;
89. Cho YH, Park Y-G, Kim S, et al. 3D Electrodes for Bioelectronics. Advanced Materials. 2021;33(47):2005805; doi:10.1002/adma.202005805.
90. Wellman SM, Eles JR, Ludwig KA, et al. A materials roadmap to functional neural interface design. Advanced functional materials. 2018;28(12):1701269;
91. Yang C, Zhang H, Liu Y, et al. Kirigami-Inspired Deformable 3D Structures Conformable to Curved Biological Surface. Advanced Science. 2018;5(12):1801070; doi:10.1002/advs.201801070.
92. Zhang W, Zhang L, Liao Y, et al. Conformal manufacturing of soft deformable sensors on the curved surface. International Journal of Extreme Manufacturing. 2021;3(4):042001; doi:10.1088/2631-7990/ac1158.
93. Goh GL, Zhang H, Chong TH, et al. 3D Printing of Multilayered and Multimaterial Electronics: A Review. Advanced Electronic Materials. 2021;7(10):2100445; doi:10.1002/aelm.202100445.
94. Shweta A, Guo Liang G, Wai Yee Y. Aerosol jet printed pH sensor based on carbon nanotubes for flexible electronics. Proceedings of the 3rd International Conference on Progress in Additive Manufacturing (PRO-AM); Singapore: Nanyang Technological University; 2018. p. 88-94.
95. Sinha AK, Goh GL, Yeong WY, et al. Ultra-Low-Cost, Crosstalk-Free, Fast-Responding, Wide-Sensing-Range Tactile Fingertip Sensor for Smart Gloves. Advanced Materials Interfaces. 2022;9(21):2200621; doi:10.1002/admi.202200621.
96. Simon DT, Gabrielsson EO, Tybrandt K, et al. Organic Bioelectronics: Bridging the Signaling Gap between Biology and Technology. Chemical Reviews. 2016;116(21):13009-41; doi:10.1021/acs.chemrev.6b00146.
97. Lee D, Jung WH, Lee S, et al. Ionic contrast across a lipid membrane for Debye length extension: towards an ultimate bioelectronic transducer. Nature Communications. 2021;12(1):3741; doi:10.1038/s41467-021-24122-8.
98. Goh GL, Tay MF, Lee JM, et al. Potential of Printed Electrodes for Electrochemical Impedance Spectroscopy (EIS): Toward Membrane Fouling Detection. Advanced Electronic Materials. 2021;7(10):2100043; doi:10.1002/aelm.202100043.

99. Ma X, Jiang Z, Lin Y. Flexible energy storage devices for wearable bioelectronics. Journal of Semiconductors. 2021;42(10):101602; doi:10.1088/1674-4926/42/10/101602.
100. Guillemot F, Mironov V, Nakamura M. Bioprinting is coming of age: Report from the International Conference on Bioprinting and Biofabrication in Bordeaux (3B'09). Biofabrication. 2010;2(1):010201; doi:10.1088/1758-5082/2/1/010201.
101. Korpela J, Kokkari A, Korhonen H, et al. Biodegradable and bioactive porous scaffold structures prepared using fused deposition modeling. Journal of Biomedical Materials Research Part B-Applied Biomaterials. 2013;101B(4):610-9; doi:10.1002/jbm.b.32863.
102. Yeong WY, Sudarmadji N, Yu HY, et al. Porous polycaprolactone scaffold for cardiac tissue engineering fabricated by selective laser sintering. Acta Biomater. 2010;6(6):2028-34; doi:10.1016/j.actbio.2009.12.033.
103. Melchels FPW, Feijen J, Grijpma DW. A poly(D,L-lactide) resin for the preparation of tissue engineering scaffolds by stereolithography. Biomaterials. 2009;30(23-24):3801-9; doi:10.1016/j.biomaterials.2009.03.055.
104. Lee JM, Sing SL, Zhou M, et al. 3D bioprinting processes: A perspective on classification and terminology. 2018. 2018;4(2); doi:10.18063/ijb.v4i2.151.
105. Odde DJ, Renn MJ. Laser-guided direct writing for applications in biotechnology. Trends in Biotechnology. 1999;17(10):385-9; doi:10.1016/S0167-7799(99)01355-4.
106. Abeyewickreme A, Kwok A, McEwan JR, et al. Bio-electrospraying embryonic stem cells: interrogating cellular viability and pluripotency. Integr Biol-Uk. 2009;1(3):260-6; doi:Doi 10.1039/B819889f.
107. Fang Y, Frampton JP, Raghavan S, et al. Rapid generation of multiplexed cell cocultures using acoustic droplet ejection followed by aqueous two-phase exclusion patterning. Tissue Eng Part C Methods. 2012;18(9):647-57; doi:10.1089/ten.TEC.2011.0709.
108. Xu T, Zhao W, Zhu JM, et al. Complex heterogeneous tissue constructs containing multiple cell types prepared by inkjet printing technology. Biomaterials. 2013;34(1):130-9; doi:10.1016/j.biomaterials.2012.09.035.
109. Guillemot F, Guillotin B, Fontaine A, et al. Laser-assisted bioprinting to deal with tissue complexity in regenerative medicine. Mrs Bull. 2011;36(12):1015-9; doi:Doi 10.1557/Mrs.2011.272.
110. Guillotin B, Souquet A, Catros S, et al. Laser assisted bioprinting of engineered tissue with high cell density and microscale organization. Biomaterials. 2010;31(28):7250-6; doi:DOI 10.1016/j.biomaterials.2010.05.055.
111. Gaebel R, Ma N, Liu J, et al. Patterning human stem cells and endothelial cells with laser printing for cardiac regeneration. Biomaterials. 2011;32(35):9218-30; doi:10.1016/j.biomaterials.2011.08.071.
112. Lee W, Lee V, Polio S, et al., editors. Three-dimensional cell-hydrogel printer using electromechanical microvalve for tissue engineering. Solid-State Sensors, Actuators and Microsystems Conference, 2009 TRANSDUCERS 2009 International; 2009: IEEE.
113. Ahn S, Lee H, Kim G. Functional cell-laden alginate scaffolds consisting of core/shell struts for tissue regeneration. Carbohydr Polym. 2013;98(1):936-42; doi:10.1016/j.carbpol.2013.07.008.
114. Billiet T, Gevaert E, De Schryver T, et al. The 3D printing of gelatin methacrylamide cell-laden tissue-engineered constructs with high cell viability. Biomaterials. 2014;35(1):49-62; doi:10.1016/j.biomaterials.2013.09.078.
115. Duan B, Hockaday LA, Kang KH, et al. 3D bioprinting of heterogeneous aortic valve conduits with alginate/gelatin hydrogels. Journal of Biomedical Materials Research Part A. 2013;101(5):1255-64; doi:10.1002/jbm.a.34420.
116. Fedorovich NE, Wijnberg HM, Dhert WJ, et al. Distinct tissue formation by heterogeneous printing of osteo- and endothelial progenitor cells. Tissue Eng Part A. 2011;17(15-16):2113-21; doi:10.1089/ten.TEA.2011.0019.

117. Huang Y, He K, Wang X. Rapid prototyping of a hybrid hierarchical polyurethane-cell/hydrogel construct for regenerative medicine. Mater Sci Eng C Mater Biol Appl. 2013;33(6):3220-9; doi:10.1016/j.msec.2013.03.048.
118. Lee H, Ahn S, Bonassar LJ, et al. Cell-laden poly(varepsilon-caprolactone)/alginate hybrid scaffolds fabricated by an aerosol cross-linking process for obtaining homogeneous cell distribution: fabrication, seeding efficiency, and cell proliferation and distribution. Tissue Eng Part C Methods. 2013;19(10):784-93; doi:10.1089/ten.TEC.2012.0651.
119. Ozbolat IT, Chen H, Yu Y. Development of 'Multi-arm Bioprinter' for hybrid biofabrication of tissue engineering constructs. Robotics and Computer-Integrated Manufacturing. 2014;30(3):295-304; doi:10.1016/j.rcim.2013.10.005.
120. Shim J-H, Lee J-S, Kim JY, et al. Bioprinting of a mechanically enhanced three-dimensional dual cell-laden construct for osteochondral tissue engineering using a multi-head tissue/organ building system. Journal of Micromechanics and Microengineering. 2012;22(8):085014; doi:10.1088/0960-1317/22/8/085014.
121. Snyder JE, Hamid Q, Wang C, et al. Bioprinting cell-laden matrigel for radioprotection study of liver by pro-drug conversion in a dual-tissue microfluidic chip. Biofabrication. 2011;3(3):034112; doi:10.1088/1758-5082/3/3/034112.
122. Wang XH, Yan YN, Pan YQ, et al. Generation of three-dimensional hepatocyte/gelatin structures with rapid prototyping system. Tissue Eng. 2006;12(1):83-90; doi:DOI 10.1089/ten.2006.12.83.
123. Skardal A, Zhang J, Prestwich GD. Bioprinting vessel-like constructs using hyaluronan hydrogels crosslinked with tetrahedral polyethylene glycol tetracrylates. Biomaterials. 2010;31(24):6173-81; doi:10.1016/j.biomaterials.2010.04.045.
124. Visser J, Peters B, Burger TJ, et al. Biofabrication of multi-material anatomically shaped tissue constructs. Biofabrication. 2013;5(3):035007; doi:10.1088/1758-5082/5/3/035007.
125. Lee JM, Yeong WY. Engineering macroscale cell alignment through coordinated toolpath design using support-assisted 3D bioprinting. Journal of The Royal Society Interface. 2020;17(168):20200294; doi:doi:10.1098/rsif.2020.0294.
126. Zhang YS, Haghiashtiani G, Hübscher T, et al. 3D extrusion bioprinting. Nature Reviews Methods Primers. 2021;1(1):75; doi:10.1038/s43586-021-00073-8.
127. Soman P, Chung PH, Zhang AP, et al. Digital Microfabrication of User-Defined 3D Microstructures in Cell-Laden Hydrogels. Biotechnol Bioeng. 2013;110(11):3038-47; doi:Doi 10.1002/Bit.24957.
128. Fedorovich NE, Oudshoorn MH, van Geemen D, et al. The effect of photopolymerization on stem cells embedded in hydrogels. Biomaterials. 2009;30(3):344-53; doi:10.1016/j.biomaterials.2008.09.037.
129. Tseng H, Gage JA, Shen T, et al. A spheroid toxicity assay using magnetic 3D bioprinting and real-time mobile device-based imaging. Scientific Reports. 2015;5:13987; doi:10.1038/srep13987.
130. Kivilcim B, Wonjin J, Wei S, et al. The role of printing parameters and scaffold biopolymer properties in the efficacy of a new hybrid nano-bioprinting system. Biofabrication. 2009;1(3):035003;
131. Nahmias Y, Odde DJ. Micropatterning of living cells by laser-guided direct writing: application to fabrication of hepatic endothelial sinusoid-like structures. Nature Protocols. 2006;1(5):2288-96; doi:10.1038/nprot.2006.386.
132. Moldovan NI, Hibino N, Nakayama K. Principles of the Kenzan Method for Robotic Cell Spheroid-Based Three-Dimensional Bioprinting<sup/>. Tissue Eng Part B Rev. 2017;23(3):237-44; doi:10.1089/ten.TEB.2016.0322.
133. Daly AC, Davidson MD, Burdick JA. 3D bioprinting of high cell-density heterogeneous tissue models through spheroid fusion within self-healing hydrogels. Nature Communications. 2021;12(1):753; doi:10.1038/s41467-021-21029-2.

134. Lee JM, Sing SL, Zhou M, et al. 3D bioprinting processes: A perspective on classification and terminology. Int J Bioprint. 2018;4(2):151; doi:10.18063/IJB.v4i2.151.
135. Wang Z, Torigoe Y, Hirai S. A Prestressed Soft Gripper: Design, Modeling, Fabrication, and Tests for Food Handling. IEEE Robotics and Automation Letters. 2017;2(4):1909-16; doi:10.1109/lra.2017.2714141.
136. Wang Y, Lee S, Wang H, et al. Robust, self-adhesive, reinforced polymeric nanofilms enabling gas-permeable dry electrodes for long-term application. Proceedings of the National Academy of Sciences. 2021;118(38);
137. Ershad F, Thukral A, Yue J, et al. Ultra-conformal drawn-on-skin electronics for multifunctional motion artifact-free sensing and point-of-care treatment. Nature communications. 2020;11(1):1-13;
138. Oh TI, Kim TE, Yoon S, et al. Flexible electrode belt for EIT using nanofiber web dry electrodes. Physiological Measurement. 2012;33(10):1603;
139. Graham B, Adler A. Electrode placement configurations for 3D EIT. Physiological measurement. 2007;28(7):S29;
140. Khan TA, Ling SH. Review on electrical impedance tomography: Artificial intelligence methods and its applications. Algorithms. 2019;12(5):88;
141. Harrison RR. The Design of Integrated Circuits to Observe Brain Activity. Proceedings of the IEEE. 2008;96(7):1203-16; doi:10.1109/JPROC.2008.922581.
142. Robinson DA. The electrical properties of metal microelectrodes. Proceedings of the IEEE. 1968;56(6):1065-71; doi:10.1109/PROC.1968.6458.
143. Wise KD, Angell JB. A Low-Capacitance Multielectrode Probe for Use in Extracellular Neurophysiology. IEEE Transactions on Biomedical Engineering. 1975;BME-22(3):212-9; doi:10.1109/TBME.1975.324562.
144. Harrison RR, editor A Versatile Integrated Circuit for the Acquisition of Biopotentials. 2007 IEEE Custom Integrated Circuits Conference; 2007 16-19 Sept. 2007.
145. Merrill DR, Bikson M, Jefferys JG. Electrical stimulation of excitable tissue: design of efficacious and safe protocols. J Neurosci Methods. 2005;141(2):171-98; doi:10.1016/j.jneumeth.2004.10.020.
146. Wagenaar DA, Pine J, Potter SM. Effective parameters for stimulation of dissociated cultures using multi-electrode arrays. J Neurosci Methods. 2004;138(1-2):27-37; doi:10.1016/j.jneumeth.2004.03.005.
147. Bontorin G, Garenne A, Lopez C, et al. Design of a bioelectronics hybrid system in real time and in closed loop. Electronics. 2012;16(2):136-44;
148. Bhave G, Chen JC, Singer A, et al. Distributed sensor and actuator networks for closed-loop bioelectronic medicine. Materials Today. 2021;46:125-35; doi:10.1016/j.mattod.2020.12.020.
149. Selberg J, Jafari M, Bradley C, et al. Expanding biological control to bioelectronics with machine learning. APL Materials. 2020;8(12):120904; doi:10.1063/5.0027226.
150. Malekpour A, Chen X. Printability and Cell Viability in Extrusion-Based Bioprinting from Experimental, Computational, and Machine Learning Views. Journal of Functional Biomaterials. 2022;13(2):40;
151. Bertoli L. In-situ monitoring of extrusion-based additive manufacturing processes via image analysis and supervised machine learning. 2020;
152. Ruberu K, Senadeera M, Rana S, et al. Coupling machine learning with 3D bioprinting to fast track optimisation of extrusion printing. Applied Materials Today. 2021;22:100914; doi:10.1016/j.apmt.2020.100914.
153. Shi J, Song J, Song B, et al. Multi-Objective Optimization Design through Machine Learning for Drop-on-Demand Bioprinting. Engineering. 2019;5(3):586-93; doi:10.1016/j.eng.2018.12.009.

154. Wu D, Xu C. Predictive Modeling of Droplet Formation Processes in Inkjet-Based Bioprinting. Journal of Manufacturing Science and Engineering. 2018;140(10); doi:10.1115/1.4040619.
155. Guan J, You S, Xiang Y, et al. Compensating the cell-induced light scattering effect in light-based bioprinting using deep learning. Biofabrication. 2021;14(1):015011; doi:10.1088/1758-5090/ac3b92.
156. Xu H, Liu Q, Casillas J, et al. Prediction of cell viability in dynamic optical projection stereolithography-based bioprinting using machine learning. Journal of Intelligent Manufacturing. 2022;33(4):995-1005; doi:10.1007/s10845-020-01708-5.
157. Goh GL, Zhang H, Goh GD, et al. Multi objective optimization of intense pulsed light sintering process for aerosol jet printed thin film. Materials Sciences in Additive Manufacturing. 2022;1(2):8; doi:10.18063/msam.v1i2.8.
158. Zhang H, Choi JP, Moon SK, et al. A hybrid multi-objective optimization of aerosol jet printing process via response surface methodology. Additive Manufacturing. 2020;33:101096; doi:10.1016/j.addma.2020.101096.
159. Jin Z, Zhang Z, Shao X, et al. Monitoring Anomalies in 3D Bioprinting with Deep Neural Networks. ACS Biomaterials Science & Engineering. 2021; doi:10.1021/acsbiomaterials.0c01761.
160. Jin Z, Zhang Z, Gu GX. Autonomous in-situ correction of fused deposition modeling printers using computer vision and deep learning. Manufacturing Letters. 2019;22:11-5; doi:10.1016/j.mfglet.2019.09.005.
161. Goh GD, Hamzah NMB, Yeong WY. Anomaly Detection in Fused Filament Fabrication Using Machine Learning. 3D Printing and Additive Manufacturing. 2022; doi:10.1089/3dp.2021.0231.
162. Nadernezhad A, Groll J. Machine learning to explain printability induced by rheology additives. ChemRxiv. 2021; doi:10.26434/chemrxiv-2021-41mn8
163. Selberg J, Jafari M, Mathews J, et al. Machine Learning-Driven Bioelectronics for Closed-Loop Control of Cells. Advanced Intelligent Systems. 2020;2(12):2000140; doi:10.1002/aisy.202000140.
164. Jafari M, Marquez G, Selberg J, et al. Feedback Control of Bioelectronic Devices Using Machine Learning. IEEE Control Systems Letters. 2021;5(4):1133-8; doi:10.1109/LCSYS.2020.3015597.
165. Jia M, Ray S, Breault R, et al. Control of pH in bioelectronics and applications. APL Materials. 2020;8(12):120704; doi:10.1063/5.0027464.
166. Williamson JR, Bliss DW, Browne DW, et al. Seizure prediction using EEG spatiotemporal correlation structure. Epilepsy & Behavior. 2012;25(2):230-8; doi:10.1016/j.yebeh.2012.07.007.
167. Li S, Zhou W, Yuan Q, et al. Seizure Prediction Using Spike Rate of Intracranial EEG. IEEE Transactions on Neural Systems and Rehabilitation Engineering. 2013;21(6):880-6; doi:10.1109/TNSRE.2013.2282153.
168. Zheng Y, Wang G, Li K, et al. Epileptic seizure prediction using phase synchronization based on bivariate empirical mode decomposition. Clinical Neurophysiology. 2014;125(6):1104-11; doi:10.1016/j.clinph.2013.09.047.
169. Bandarabadi M, Teixeira CA, Rasekhi J, et al. Epileptic seizure prediction using relative spectral power features. Clinical Neurophysiology. 2015;126(2):237-48; doi:10.1016/j.clinph.2014.05.022.
170. Park Y, Luo L, Parhi KK, et al. Seizure prediction with spectral power of EEG using cost-sensitive support vector machines. Epilepsia. 2011;52(10):1761-70; doi:10.1111/j.1528-1167.2011.03138.x.
171. Bian L, Wang Z, White DL, et al. Machine learning-assisted calibration of Hg2+ sensors based on carbon nanotube field-effect transistors. Biosensors and Bioelectronics. 2021;180:113085; doi:10.1016/j.bios.2021.113085.
172. Zhang Y, Tao TH. Skin-Friendly Electronics for Acquiring Human Physiological Signatures. Advanced Materials. 2019;31(49):1905767; doi:10.1002/adma.201905767.

173. Rodeheaver N, Herbert R, Kim Y-S, et al. Strain-Isolating Materials and Interfacial Physics for Soft Wearable Bioelectronics and Wireless, Motion Artifact-Controlled Health Monitoring. Advanced Functional Materials. 2021;31(36):2104070; doi:10.1002/adfm.202104070.
174. Kwon Y-T, Kim Y-S, Kwon S, et al. All-printed nanomembrane wireless bioelectronics using a biocompatible solderable graphene for multimodal human-machine interfaces. Nature Communications. 2020;11(1):3450; doi:10.1038/s41467-020-17288-0.
175. Kwon Y-T, Kim H, Mahmood M, et al. Printed, Wireless, Soft Bioelectronics and Deep Learning Algorithm for Smart Human–Machine Interfaces. ACS Applied Materials & Interfaces. 2020;12(44):49398-406; doi:10.1021/acsami.0c14193.
176. Moon G, Choi J-r, Lee C, et al. Machine learning-based design of meta-plasmonic biosensors with negative index metamaterials. Biosensors and Bioelectronics. 2020;164:112335; doi:10.1016/j.bios.2020.112335.
177. Chen A, Zhang J, Zhao L, et al. Machine-learning enabled wireless wearable sensors to study individuality of respiratory behaviors. Biosensors and Bioelectronics. 2021;173:112799; doi:10.1016/j.bios.2020.112799.
178. Mahmood M, Kwon S, Berkmen GK, et al. Soft Nanomembrane Sensors and Flexible Hybrid Bioelectronics for Wireless Quantification of Blepharospasm. IEEE Transactions on Biomedical Engineering. 2020;67(11):3094-100; doi:10.1109/TBME.2020.2975773.
179. Mahmood M, Kim N, Mahmood M, et al. VR-enabled portable brain-computer interfaces via wireless soft bioelectronics. Biosensors and Bioelectronics. 2022;210:114333; doi:10.1016/j.bios.2022.114333.
180. An S, Pu X, Zhou S, et al. Deep Learning Enabled Neck Motion Detection Using a Triboelectric Nanogenerator. ACS Nano. 2022;16(6):9359-67; doi:10.1021/acsnano.2c02149.
181. Kim KK, Ha I, Kim M, et al. A deep-learned skin sensor decoding the epicentral human motions. Nature Communications. 2020;11(1):2149; doi:10.1038/s41467-020-16040-y.
182. Halilaj E, Rajagopal A, Fiterau M, et al. Machine learning in human movement biomechanics: Best practices, common pitfalls, and new opportunities. Journal of Biomechanics. 2018;81:1-11; doi:10.1016/j.jbiomech.2018.09.009.
183. Finn C, Abbeel P, Levine S, editors. Model-agnostic meta-learning for fast adaptation of deep networks. International conference on machine learning; 2017: PMLR.
184. Pan SJ, Yang Q. A Survey on Transfer Learning. IEEE Transactions on Knowledge and Data Engineering. 2010;22(10):1345-59; doi:10.1109/TKDE.2009.191.

List of Figures

Figure 1: (a) Flowchart for supervised learning, unsupervised learning, and reinforcement learning. (b) Examples for various approaches of machine learning

Figure 2 (a) Schematic for deep neural network (DNN). (b) Schematic for recurrent neural network (RNN). (c) Schematic for convolutional neural networks (CNN), the architecture shown is LeNet-5 [26].

Figure 3 A closed-loop bioelectronic system with the ML-control of bioelectronic actuators using sensor feedback. Adapted with permission from [103] . Copyright 2020, AIP Publishing.

Figure 4 a) System to be optimized b) Bayesian Optimisation framework [106].

Figure 5 (a,b) Bar charts showing anomaly information for both full and testing data sets. The number of labels for three types of anomalies under four infill patterns is shown. (c) Flow diagram showing the architectures of applied CNN models. The self-designed CNN architecture is illustrated at the top, and the pretrained model is shown at the bottom. (d) Anomaly detection result visualization on test data. Adapted with permission from [113]. Copyright 2021, American Chemical Society.

Figure 6 (a) The multi-level control system and its main components (i.e., the decision-maker, planner, and low-level controller) and its robustness to uncertainties, noise, and unmodeled dynamics. (b) Machine learning-based system for Vmem control using pH modifying bioelectronics and fluorescence feedback. Adapted with permission from [103] . Copyright 2020, AIP Publishing.

Figure 7 a) Drawing illustrating specific muscles on forearm to detect various hand postures and photos capturing three p-NHE placed on specific muscles, including palmaris longus, brachioradialis, and flexor carpi ulnaris. B) EMG mapping data illustrating RMS signals from multiple channels that encompasses the whole forearm; six different heat maps are generated based on six gestures. C) Representative EMG signals from four gestures, including open hand, closed hand and index finger flexion and wrist flexion. D) Demo of EMG-enabled human-machine interfaces with a wireless, wearable p-NHE to precisely control a flying drone, RC car, and presentation software. E) 3D plot of three-channel, EMG RMS signals for clear differentiation of seven different gestures as seven groups. F) Result of real-time, confusion matrix from ten trials, showing 98.6% accuracy across seven classes with three-channel EMG recording. G) Demo of a three-channel EMG recording and corresponding control of a robotic hand, demonstrating examples of six motions of a subject and following motions of the robotic hand. Reprinted with permission from [128]. Copyright 2020, Nature.

Figure 8 (A) Wireless wearable sensors positioned on the midway of the xiphoid process and the costal margin, one on each location, corresponding to the abdomen-apposed rib cage, and 1 cm above the umbilicus, respectively.(B) Picture of the fabricated wireless wearable sensor on a flexible polyimide substrate. (C) Respiratory behaviors data obtained from four postures of subjects were input to a ML algorithm. (D) ML algorithm process flow.

List of Tables